2020

MODELING AND EXPERIMENTAL TESTING OF SOLAR POWERED INJERA BAKING

ANEMUTE, YOHANES

BAHIR DAR UNIVERSITY

BAHIR DAR INSTITUTE OF TECHNOLOGY

SCHOOL OF RESEARCH AND POST GRADUATE STUDIES

FACULTY OF MECHANICAL AND INDUSTRIAL ENGINEERING

MODELING AND EXPERIMENTAL TESTING OF SOLAR POWERED INJERA BAKING

YOHANES ANEMUTE

Bahir Dar, Ethiopia

September 21, 2020

MODELING AND EXPERIMENTAL TESTING OF SOLAR POWERED INJERA BAKING

YOHANES ANEMUTE

A Thesis submitted to the school of Research and Graduate Studies of Bahir Dar

Institute of Technology, Bahir Dar University in partial fulfillment of the requirements for

the degree of

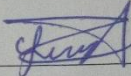Master in Thermal Engineering in Faculty of Mechanical and Industrial Engineering

Adviser Name: Dr. Bimrew Tamrat

Bahir Dar, Ethiopia

September 21, 2020

DECLARATION

I, the undersigned, declare that the thesis comprises my own work. In compliance with internationally accepted practices, I have acknowledged and refereed all materials used in this work. I understand that non-adherence to the principles of academic honesty and integrity, misrepresentation/ fabrication of any idea/data/fact/source will constitute sufficient ground for disciplinary action by the University and can also evoke penal action from the sources which have not been properly cited or acknowledged.
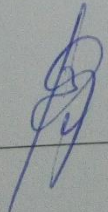
Name of the student _Yohanes Anemute_ Signature _____

Date of submission: _____

Place: Bahir Dar

This thesis has been submitted for examination with my approval as a university advisor.

Advisor Name: _Bimrew T. (Ph D)_

Advisor's Signature: _____

Bahir Dar Institute of Technology-Bahir Dar University

School of Research and Graduate Studies

Faculty of Mechanical and Industrial Engineering

THESIS APPROVAL SHEET

Student:

Yohanes Anemute _____ 16/09/2020

Name   Signature   Date

The following graduate faculty members certify that this student has successfully presented the necessary written final thesis and oral presentation for partial fulfillment of the thesis requirements for the Degree of Master of Science in thermal engineering.

Approved By:

Advisor: Bimrew Tamrat (PhD) _____ 22/09/2020

Name   Signature   Date

External Examiner: Abdulkadir Aman(PhD) _____ 09/09/2020

Name   Signature   Date

Internal Examiner: Muluken Temesfa _____ 09/09/2020

Name   Signature   Date

Chair Holder: Temesgen Assefa _____ 22/09/2020

Name   Signature   Date

ሮቤል ንጉሴ ወርቅአለማሁ
Robel Nigussie Workalemahu
ፋኩልቲ ዲን
Faculty Dean

Faculty Dean: _____ 22/09/2020

Name   Signature   Date

iii

ACKNOWLEDGEMENTS

ABSTRACT

Ethiopia is the country which use fossil fuel as main source of energy. About 83% people of the country live in countryside area and use fossil fuel as a source energy for any baking and cooking purpose. Among this 70% of the energy is used for baking injera which needs a high temperature in range of 180-220℃ in a control environment. Thus, substituting it by renewable energy is an admirable solution of the season. The work of this thesis proves it is possible and propose new type of baking system with renewable energy source in indoor baking mechanism using solar thermal energy source of power. The possibility for baking injera is investigated using thermal energy transfer to thermal storage and baking pan by means of circulating heat transfer fluid (HTF) heated by parabolic dish solar collector. The existing three stone baking pan and electric pan causes environmental pollution, healthy affection, much amount of energy lose and in accessible in rural area.

The thermal energy is collected using $2m^2$ area parabolic dish collector to the heat transfer fluid through spiral coil copper absorber and the hot HTF flow and placed to a hot oil container volume of 16litters which is covered by solar salt ($60\%NaNO_3/40\%KNO_3$) properly insulated by wood ash. The fluid stored in hot oil storage flow baking pan with 0.5m diameter and 5mm thickness when baking is required and allow flow to cold oil storage after a pan absorbs heat from the HTF and circulate bake to spiral copper coil receiver to heat up again. There is metal plate between the clay pan and the fluid to avoid cracking of pan by hot HTF. The experimental setup is manufactured from locally available material. Leakage of fluid was difficult to control during experimental test. Instruments like thermo couple, infrared thermometer and Pyranometer are used in the experimental test. Thus, HTF is heated by parabolic dish collector at the absorber plate and attain up to a temperature of 253℃ and the average day thermal efficiency was around 51.44 %. Using the fluid temperature as an input data and manipulating using MATLAB software the upper surface temperature of the baking pan raised up to 210℃ which is absolutely enough to bake injera and the first heat up time was around 10minutes and the retaining time after one lap was 3minutes. Finally, the correlation of the parameter was developing by sigma plot.

Key words: baking pan, solar thermal, heat transfer fluid, PCM, parabolic dish, spiral coil

TABLE CONTENTS

LIST OF SYMBOLS

A	Area of the pan
A_a	Aperture area of the dish ()
A_{abs}	Absorber area
A_{sc}	Heat transfer area of spiral coil
A_r	Area of receiver
C	Concentration ratio
C_p	Specific heat capacity water
D	diameter of the pan (m)
D	diameter of dish (m)
F	focal point of dish
F	Load
h	convection heat transfer coefficient
H	height of the dish (m)
I_b	Beam radiation
I_d	Long-term average direct radiation
K	Thermal conductivity
K_{pl}	Thermal conductivity of supporting plate carbon steel
K_p	Thermal conductivity of cooking pan
l	effective length of the heat transfer
m_{Injera}	mass of Injera baked (g)
Nu	Nusselt number
P	power required for baking (w)

Pr-	Pradtel number
Q	heat energy (kJ)
Q_{abs}	Absorber heat energy
Q_{total}	total heat required
Q_u	Useful heat energy
Ra	Raleigh number
R	radius (m)
T_1	Initial temperature ($^\circ$ C)
T_2	Final temperature ($^\circ$ C)
t_1	Supporting sheet metal thickness (m)
t_2	Thickness of baking pan (m)
T_{fm}	Fluid mean temperature

GREEK LETTER

α	Thermal diffusivity
β	Coefficient of thermal expansion
ρ	Density of clay
μ	Dynamic viscosity
υ	Kinematics' viscosity
ρ	Reflectivity
α	Absorbance

LIST OF ABREVATIONS

CSP   Concentrated Solar Power

HTF   Heat Transfer Fluid

EELPA   Ethiopian Electric Light & Power Authority

NASA   National Aeronautics and Space Administration

PCM   Phase Change Material

TES   Thermal Energy Storage

TCS   Thermo-Chemical Storage

LIST OF FIGURE

LIST OF TABLES

CHAPTER ONE

1   INTRODUCTION

1.1   Background

The development of one country depend on the availability of adequate amount of energy and development is imaginable over an increasing efficient consumption and extensive harnessing of different forms of energy. Suffering in energy disaster is common in most developing, which is

characterized by reduction of locally accessible energy resources and reliance on imported fuels. The energy disaster is increasing the food trouble by increasing the rate of deforestation and thereby causing degradation of farmlands. Additionally, requirement on imported fuel is weakening the capacity of the concerned countries to buy food whenever the need arises. Despite rapid urbanization, the majority of Ethiopians still live in rural areas, and access to and utilization of energy resources varies considerably thorough the country. Although Ethiopia has huge potential for emerging numerous energy resources, but the per capital energy consumption remains to be among the least in the world[1].

The accessibility of suitable energy for household cooking is one of the most important anxieties of people in Ethiopia. Ethiopians' high dependence on biomass energy resources contribute to deforestation, soil erosion, and land degradation. The conventional energy sources are inadequate and quickly becoming depleted with time; on the other hand, rapid increasing population and growing human activities are applying additional pressure with extra demand on the shrinking amount of energy resources[2].

Injera is flat bread with a unique taste and texture [3]. It is mainly eaten as the first choice food item in Ethiopia and some parts of East Africa. Injera baking requires temperatures ranging from 180°C – 220°C [4]. In most households of Ethiopia, the energy demand for baking Injera is largely met with bio-fuels such as fuel wood, agricultural residue and dung cakes, whereas electricity is used in some of the urban households. In most households, this Injera baking system is carried out using an open fire / three stone) baking system which are inefficient and wasteful techniques. One serious disadvantage of this method is that it consumes considerable quantities of firewood, estimated to be at least 50 % of the biomass energy consumption per household per year. Though

the use of electricity for Injera baking is limited to urban inhabitants, the Injera baking electrical mitad contributes to large energy consumption in the electricity supply system of the country[1]. It is widely perceived that the efficiency for energy consumption of the existing electrical mitad is low arising from old design and its manufacturing defaults. The current mitad design dates back to 1960's when baking of Injera electrical mitad started with high-income groups in cities. However, since then, almost no design improvements have taken place (Dave, 2010). Furthermore, since electrical mitad is manufactured traditionally with untrained workers, it is expected that it will have lower energy consumption efficiency hence a wider room for improvement. To improve health and general welfare, better cooking and heating facilities are important. Solar cooking can decrease the health hazards associated with indoor fire cooking and the economic burdens associated with fire-wood gathering or purchase[3].

1.2 Statement of problem

The availability of adequate energy for household cooking is important concerns. Food cooking especially baking process is an energy intensive unit operation and it becomes more challenging for the developing countries facing severe energy crises. The conventional energy sources are limited and rapidly becoming depleted with time; on the other hand, rapid population growth and expanding human activities are exerting extra pressure with additional demand on the shrinking

amount of energy resources. Ethiopian is highly dependence on biomass energy resources. This contribute to deforestation, soil erosion, and land degradation.

To mitigate the problem, use of alternative source of energy is peremptory issue. Since Injera baking is a traditional food of Ethiopians and some east African countries, there is no adequate research works related to its baking system. But there are few researches which are done by Ethiopian researchers. Among those works steam based solar powered injera baking, solar parabolic through injera baking and glass pan baking system are studied. Still a continuous improvement is needed.

The aim of this work is modeling and experimental testing on solar power injera baking by: adding thermal storage system, improving heat transfer rate from fluid to pan and reduce energy loses of the working fluid. The experiment is conducted using parabolic dish as a solar collector and its result is evaluated using MATLAB and SIGMA PLOT.

1.3   Objective of the study

1.4   General objective

The general objective the study is modeling, manufacturing and experimental testing of solar powered Injera baking

1.5   Specific objective

The specific objectives of this thesis work will be to:

- Thermal analysis

- mathematical modeling of the pan

- size solar collector and select the receiver

- select appropriate working fluid

- prototyping and manufacturing of the baker

1.6 Scope of the research

This research will address from theoretical analyses and mathematical modeling of the system to simulation of the system by using software, prototyping, manufacturing and experimental test. After all, by recording the experimental data compare this work from the previous one and will show the improving work.

1.7 Significance of the research

In this work, it is expected to get an adequate amount of solar energy that can be collected using a proper solar collector which can be sufficient to bake Injera in the range of 180℃ to 220℃. Secondly, design and manufacture an efficient pan than the previous pan type which can go with the energy supply as solar energy with appropriate thermal energy storage. Finally, this work will solve serious community problem special Ethiopian rural women that exhausted for gathering biomass and healthy tricky during baking Injera by using biomass.

Energy plays an important role on the development of a nation and development is possible through an increasing efficient use and extensive harnessing of various forms of energy. Today most of the country in the world have the policy concern on the renewable energy sources. Ethiopian also the country which give a high emphasis for renewable energy. Replace high energy consuming process will have the following significant.

- It will reduce burning of high amount of fossil fuel

- It will upsurge culture of using renewable energy

- It will add a value on the capacity of national energy

- Reduce deforestation

- Environmental pollution will be reducing

- It will avoid healthy problem in women when bake Injera in biomass fuel

- Develop the emancipation of women in the society mainly in rural area of the country

CHAPTER TWO

2   LITERATURE REVIEW

2.1   Overview of Injera Baking

Injera, a processed food of different cereals, teff, millet, sorghum, maize, wheat, rice etc., or combinations of those passed through fermentation and rigorous baking process, is the widely and cultural food of some east African countries particularly Ethiopia, Eritrea and to some extent Somalia. Injera was baked most commonly on a clay plate called Mitad that is placed over a three stone stove or on specialized electric stove. When a fermented dough poured on a hot clay pan and stayed until the boiling temperature reached; bubbles from the boiling water escape forming thousands of tiny craters (eyes) that give the peculiar Injera texture. The traditional Mitad consists of a griddle plate of 'black' clay set on a base of stone and clay[4].

Most of the people living in Ethiopia bake Injera using biomass on open-fire stoves. The inefficient open fire stove consumes large amounts of fire wood and produces high indoor air pollution and CO_2 emission. A three-stone-stove or a three-stand-stove is where three stones with a similar size are made from clay. The three stones are placed in a triangle to support or carry the baking pan with a diameter of 60cm and thickness of 2cm on average. Then firewood is inserted into the openings between the stands for burning. While burning is taking place below the pan Injera is baked on it. In the process, 90% of the energy supplied is lost to the environment. Moreover, the cook and her child is exposed to large amounts of CO and PM which is above the WHO standard set for safe cooking[5].

2.2 Injera baking techniques

In Ethiopia Currently three baking techniques are used for baking Injera. These are:

1. Baking on Open fire method (three stone method)

2. Baking on Mirt-injera stove and

3. Baking on Electric baking pan

2.2.1 Three-stone-fire for baking Injera

As the name indicates, a three-stone open-fire stove uses three separate stones to support the mitad (clay pan) for baking. The types and sizes of stones used varies according to the availability of the stones. Usually three (10–15 cm) high stones are used to support the mitad.

A number of developers have used a three-stone open-fire injera baking stove as a reference for showing the improvements with various versions of the Mirt stove. The specific fuel consumption of a three-stone open-fire stove on average is 929 g of wood/kg of injera using CCT protocol for testing conducted tests on Mirt and three-stone open-fire injera baking stove and obtained indoor

air pollution parameters for three-stone open-fire stove as 80 ppm for CO and 1.10 mg/m3 for PM[4].

Figure 2.1 Three stone fire baking Injera[4]

2.2.2   Baking on Mirt-injera stove

The specific fuel consumption of Mirt stove has been determined by a number of researchers and developers. The average specific fuel consumption of Mirt stove is 535 g of wood per kg of Injera[6].

Figure 2.2 Mirt injera stove[4]

2.2.3 Baking on Electric baking pan

Electric injera baking stove (electric injera mitad) was introduced to Ethiopia 40 years (EEA, 2015) back through the then Ethiopian Electric Light & Power Authority (EELPA). In order to disseminate the electric Injera stove, various government and private organizations produced the stove and sold it to the market. Since the electric injera baking stove is not standardized, the performance of the electric injera baking stove depends on the experience of the company and the quality of the workmanship. The average power demand of a single household electric injera baking stove is in the range of 3 to 4 kW. Figure 2.3 shows a commonly manufactured electric injera baking stove. Currently, small manufacturing enterprises are involved in the manufacturing of the electric injera baking stove. The number of electric injera stove in use is estimated to reach 850,000 in the year 2020 (EEA, 2015), which demands corresponding energy efficiency measures to improve the peak hour load created by households[7].

Figure 2.3 Electric baking pan[4]

2.2.4 Solar powered injera baking stove

The 1994 Ethiopian energy policy document stipulates that alternative energy sources and technologies shall be developed to meet increasing demand and encouraged and supports adoption of renewable energy technologies. Solar energy, among renewable energy resources, can be taken

as a measure to solve the increasing house hold energy demand of the nation. So far, the Scheffler reflector systems are solar thermal systems used as Injera baking stoves. In this system the concentrating reflectors track the movement of the sun, reflecting the light of the sun and concentrating it on a fixed position. In some configurations the reflected and concentrated sunlight enters a nearby kitchen directly to strike a cooking pot or baking pan. In other configurations, the concentrated sunlight is used first to create steam which is transported by pipes to a nearby kitchen. But the second configuration is not being used for Injera baking since steam will not bring the temperature at which the baking surface of the plate requires to operate. Scheffler cookers are normally termed as community cookers, since it can provide enough heat sources for a certain group of households[8].

There are few Scheffler cookers in Ethiopia which are manufactured by Solar Bereket. but due to high cost and less efficiency the cooker is not yet fully introduced in Ethiopian market.

(a)   (b)
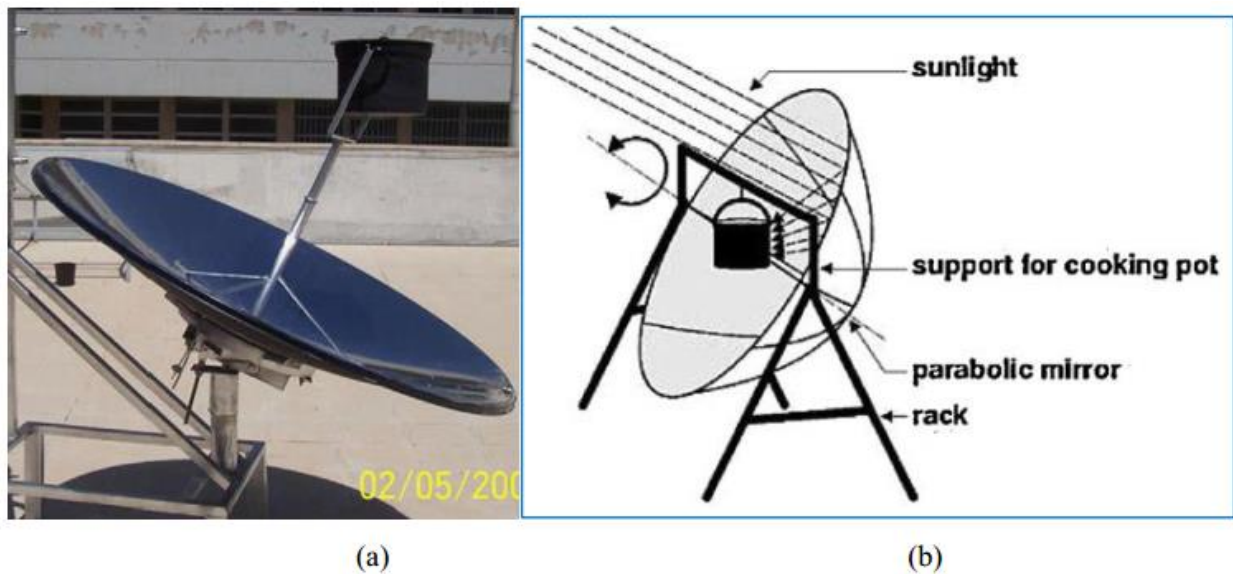
Figure 2.4 Concentrating direct solar cooker and water heater operating in the cooking mode[9]

The parabolic trough system is another method used as Injera baking stoves this method is modeled in laboratory. In this system the collector tracks the movement of the sun, reflecting the light of

the sun and concentrating it in to receiver tube that contain heat transfer fluid (oil). this heat transfer fluid also transfers in to the baking pan by using pipe. The pipe runs through and heat the clay and heat the clay and perform the baking activity. This method uses oil as heat transfer fluid for this set up set up oil is not easily available and expensive as well. It also requires special pan that have large thickness in order to run the pipe [10].

Devos cooker is another option which can be used for future solar baking stoves. It is a parabolic solar cooker with a table to protect the cook. However, many differences and advances are noticeable from the usual parabolic cooker. The cooker is made of two main parts, a table and a concentrator. The concentrator reflects and focuses the solar rays under the table, where a hole is made, and where the pot can be placed. The concentrator is asymmetrical. That way, it can collect all the solar rays. This also allows the table and the pot not to make any shadow on the concentrator. The cooker protects the cook from burns and dazzles. Even if the focus moves, the table shelters the user and is a safety device to do the cooking quietly.

There are two devices used to track the solar position. The first one allows the control and the tracking of the variation of solar azimuth. The second one allows the tracking of the variation of solar altitude. A special device can regulate the heat under the pot. A shutter and an indicator allow the cook to reduce or increase the heat under the pot. Though it doesn't allow for indoor baking purposes, Devos cookers are good options for solar thermal baking applications. Aside from cost and performance requirements, residential solar cookers must meet certain social conditions if they are to gain wide-scale acceptance. No one wants to cook in the sun, somehow the energy from the sun needs to be brought inside the kitchen. Moreover, the cooker must not require much attention in the way of adjustments and service. Lastly, using the solar cooker must not be any harder than using conventional cookers[11].

Indirect solar cookers, the split system cooker arrangement helps solar cooking inside the kitchen. These systems are made of a solar collector which is an evaporator, heat pipe which has heat transferring fluid in it and a condenser was investigated. Cylindrical parabolic collectors are capable of collecting solar radiation to a temperature of more than 400℃. This collector can be used for indoor baking option using a heat transporting fluid (salt solution), and salt solution storage tank at which the fluid will start and end its closed circulation paths[12]. Investigation for the possible use of an indoor solar thermal baking is the main target of this thesis.

2.3 Solar thermal energy

Solar energy strikes our planet a mere 8 min 20 s after leaving the sun which is 1.5×10^{11} m away. The sun's total energy output is 3.8×10^{20} MW which is equal to 63MW/m2 of the sun's surface. The world's overall solar energy resource potential is around 5.6 gigajoules (GJ) (1.6 megawatt-hours (MWh)) per square meter per year. The highest solar resource potential is in the red sea area, including Egypt and Saudi Arabia. Solar energy is the most favorable alternative energy which can serve as a substitute for fossil fuel; it is non-polluting source of energy which if properly harness and utilized can help to curtail the amount of co_2 emitted to the atmosphere due to the combustion of fossil fuel. Widespread use of solar energy for domestic, agricultural and agro-industrial activities has been practice almost since the development of civilization, the increasing threat of acute shortage of the commercial sources of energy coupled with serious environmental pollution problems has accelerated interest in the scientific exploration of renewable sources of energy. It is estimated that the small fraction of solar radiation falling on the earth is equal to the world energy demand for one year[13].

Solar energy collectors are special kind of heat exchangers that transform solar radiation energy to internal energy of the transport medium. The major component of any solar system is the solar

collector. This is a device which absorbs the incoming solar radiation, converts it into heat, and transfers this heat to a fluid (usually air, water, or oil) flowing through the collector. The solar energy thus collected is carried from the circulating fluid either directly to the hot water or space conditioning equipment, or to a thermal energy storage tank from which can be drawn for use at night and/or cloudy days[14].

2.4   Solar energy technology

There are basically two types of solar collectors: non-concentrating or stationery and concentrating. A non-concentrating collector has the same area for intercepting and for absorbing solar radiation, whereas a sun-tracking concentrating solar collector usually has concave reflecting surfaces to intercept and focus the sun's beam radiation to a smaller receiving area, thereby increasing the radiation flux.

Table 2.1 *different type of solar collectors*[9]

Motion	Collector type	Absorber type	Concentration ratio	Indicative temperature range (℃)
stationary	Flat Plate Collector (FPC)	Flat	1	30-80
	Evacuated Tube Collector (ETC)	Flat	1	50-200
	Compound Parabolic collector (CPC)	Tabular	1-5	60-240
Single-axis trucking	Linear Fresnel Reflector (LFC)	Tabular	10-40	60-250
	Parabolic Trough Collector (PTC)	Tabular	15-45	60-300
	Cylindrical Trough Collector (CTC)	Tabular	10-50	60-300
Two-axis trucking	Parabolic Dish Reflector (PDR)	Point	100-1000	100-500
	Heliostat Field Collector (HFC)	Point	100-1500	150-2000

Among different type of solar collector parabolic dish type solar collector has been consider for this work.

2.4.1 Parabolic Dish Collectors

Using parabolic dishes is a well-tested approach to concentrate solar radiation, and was an early experimental tool at many locations worldwide. The optical efficiency of parabolic dishes is considerably higher than that of parabolic trough, Linear Fresnel reflector or Power tower systems because the mirror is always pointed directly at the sun [13]. In this study, the reflector for the parabolic concentrator is made of a mirror; the interior of the parabolic concentrator is covered with the reflective mirrors, which reflect the solar rays on the face of a receiver placed at the focal position of the parabolic concentrator.

2.4.2 Design of solar parabolic concentrator

In a parabola, all the incoming solar rays from a light source are reflected back to the focal point of the parabola. The solar concentrator was developed using a semi-spherical surface covered with many small sections of mirrors to form a segmented, spherical concentrator. The frame of the parabola was made from a mini dish satellite receiver plate. The solar concentrator takes advantage of all incoming solar radiation and concentrates it at the focus[15].

Figure 2.5 shows the parabolic dish concentrator parameters. The equation for the parabola in cylindrical coordinates is given by:

$$Z = \frac{r^2}{4f}$$
2.1

The diameter of the opening parabolic surface is d, and the focal distance of the parabola is f. the surface of this parabola is given by[16]:

$$S = \left[1 + \left(\frac{d}{4f}\right)^2\right]^{\frac{3}{2}} - 1$$
2.2

14

The cross-section of the opening is: $A = \frac{\pi d^2}{4}$

To calculate the focal distance, the following equation is use

$$f = \frac{d^2}{12h}$$ 2.3
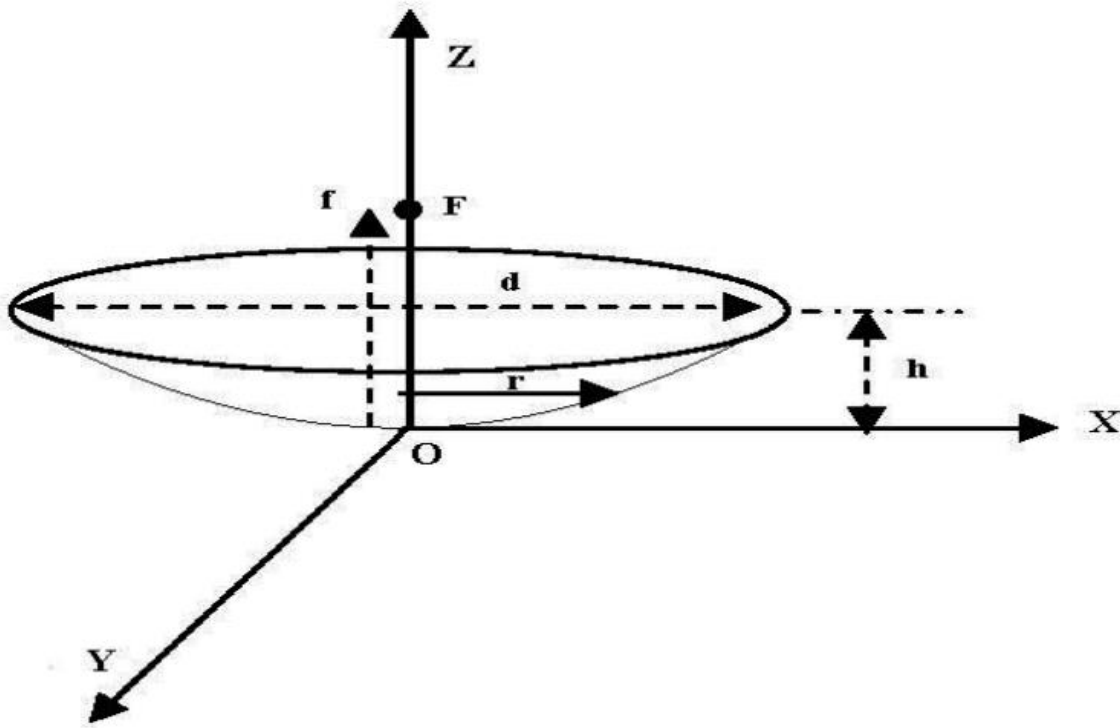
Figure 2.5 parabolic dish concentrator parameters [17]

Where

- h is the height of the dish

- d is the diameter of the dish

- f is the focal point

- F is the load

- r is the radius

2.4.3 Operating principle of parabolic dish concentrators

Concentrators are only a portion of an energy collection system. To be useful, the concentrated rays must be directed to a target called the receiver, which converts the rays into another form of energy, heat. The concentrator and receiver must be matched for optimum performance. For parabolic dish concentrator, the concentration of light is achieved with mirrors (reflection) or with transparent lens (refraction)[17]. The solar parabolic concentrator works on the principle of solar energy concentration. A very high temperature can be obtained from the system since the sun's rays are concentrated on the pot which is painted black for good absorption. The solar concentrator is very simple to operate and easy to maintain, the solar concentrator can be oriented manually to face the sun's direction. And the operating period is from 6-8 hours. The operating principle of the parabolic dish concentrator is as shown in figure 2.6.
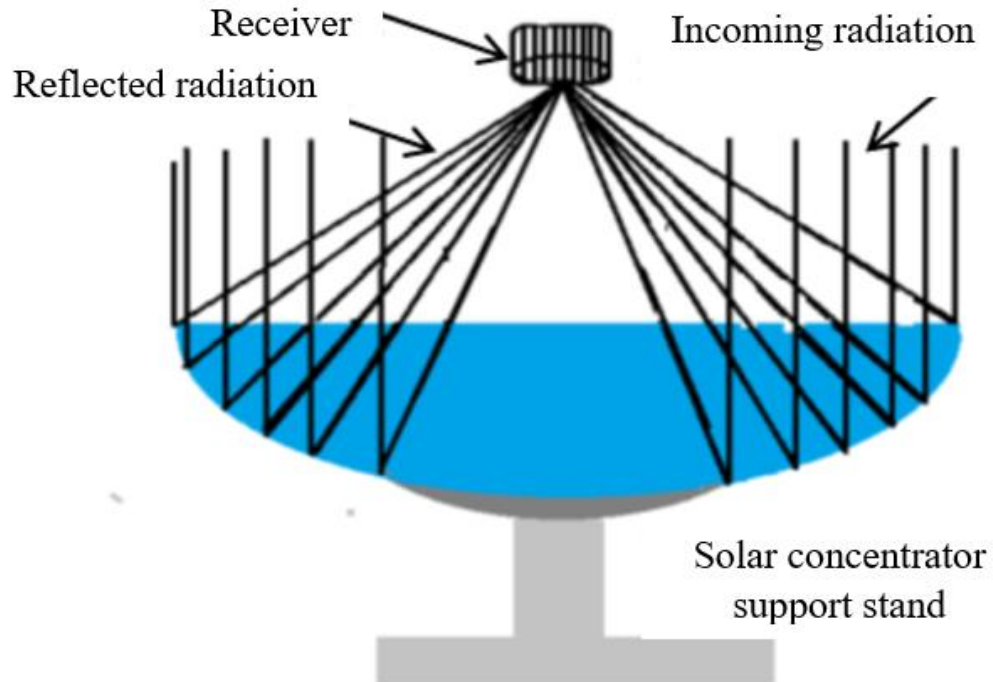
Figure 2.6 parabolic dish concentrator.[17]

16

2.4.4 Concentrating ratio

The Concentrator ratio C_R is use to describe the amount of light energy concentration achieved by a given collector. It is defining as the area of the collector aperture A_a divided by the surface area of the receiver (A_r).[15] As shown in the equation

$$C_R = \frac{A_a}{A_r}$$
  <div align="right">2.4</div>

Where; A_a is the area of the concentrator

A_r is the area of the receiver

2.4.5 Availability of solar energy in Ethiopia

The data obtained shows that tropical regions offer a better solar energy source than at more temperate latitudes. As a whole for Ethiopia the yearly average radiation reaching the ground is 5.26kwh. Even though in Ethiopia the properly recorded solar radiation data is available only for Addis Ababa (NASA, 2010), the data used in sizing and simulation is based on data recorded for more than 10 years by the NASA Surface meteorology and Solar Energy: RET Screen Data (Ansari and Mokhtar, 2005

2.5 Heat transfer fluid

HTFs can be classified by their states of matter during normal operating conditions. Additionally, to the three standard states (gaseous, liquid, solid), HTFs that undergo a phase change and supercritical fluids are also possible.

Heat transfer fluid (HTF) is a key component of concentrated solar systems that governs the working temperature of the thermo dynamical cycles.

HTF may also be used as storage medium but it is used at least to extract heat from the storage tanks. There are currently several classes of compounds that have been commercialized as heat transfer fluids see Table 2.2. The organic fluids remain liquid over a wide temperature range but

suffer from high vapor pressures and flammability that preclude their use above 300°C–400°C. In contrast, inorganic nitrate salts have good thermal stability but high freezing points.

Table 2.2Class of Heat Transfer Fluid[18]

HTF	Application temperature (°C)	Properties
Synthetic oils	13 to 340	Flammable
Mineral oils	-10 to 300	Flammable
Silicon oils	-40 to 400	Expensive flammable
Nitrate salts	220 to 500	Freezing point $\geq$ 120°C high temperature stability

2.5.1 Important thermophysical properties of HTFs

➢ Lower temperature limitation (solidification temperature)

➢ chemical compatibility (low corrosivity) with contact materials

➢ Extended working temperature range and high thermal stability.

➢ Good heat transfer properties. For instance, a large thermal conductivity (k) is desired for efficient heat transfer, and a low viscosity (μ) is beneficial to pressure drop. In addition, a large heat capacity (C_p) would allow for direct thermal storage, although indirect solutions with a secondary medium are also possible.

➢ Low vapor pressure

- ➢ low toxicity, flammability, explosivity, hazard properties and environmental and large material compatibility.

- ➢ Low cost, high availability.

2.6 Phase change material

Thermal energy storage (TES) is a technology that stores thermal energy by heating or cooling a storage medium so that the stored energy can be used at a later time for heating and cooling applications and power generation. TES systems are used particularly in buildings and industrial processes. In these applications, approximately half of the energy consumed is in the form of thermal energy, the demand for which may vary during any given day and from one day to the next. Therefore, TES systems can help to balance energy demand and supply on a daily, weekly and even seasonal basis. They can also reduce peak demand, energy consumption, CO_2 emissions and costs, while increasing overall efficiency of energy systems. Furthermore, the conversion and storage of variable renewable energy in the form of thermal energy can also help to increase the share of renewables in the energy mix. TES is becoming particularly important for electricity storage in combination with concentrating solar power (CSP) plants where solar heat can be stored for electricity production when sunlight is not available[19].

There are three kinds of TES systems, namely: 1) sensible heat storage that is based on storing thermal energy by heating or cooling a liquid or solid storage medium (e.g. water, sand, molten salts, rocks), with water being the cheapest option; 2) latent heat storage using phase change materials or PCMs (e.g. from a solid state into a liquid state); and 3) thermo-chemical storage(TCS) using chemical reactions to store and release thermal energy. Sensible heat storage is relatively inexpensive compared to PCM and TCS systems and is applicable to domestic systems, district heating and industrial needs. However, in general sensible heat storage requires large volumes

because of its low energy density (i.e. three and five times lower than that of PCM and TCS systems, respectively)

Among different types of thermal energy storage, latent heat storage type plays a vital role. Particularly, phase change materials (PCMs) absorb or release heat from the environment by changes in phase or structure, so as to realize the storage and release of thermal energy. Some studies have pointed out that the advantages of PCMs are high heat storage density, huge latent heat storage capacity, low cost, excellent chemical stability, etc. PCMs have a wide range application due to continuous research, such as industrial waste heat recovery, comfort applications in buildings, electric peak–shaving, solar energy systems, etc. In addition, PCMs have a prominent feature that the temperature nearly remains constant during phase change process, which can be used in temperature control system[20].

2.7   Thermal Insulation system

Insulations are defined as those materials or combinations of materials which retard the flow of heat energy by performing one or more of the following functions:

1. Conserve energy by reducing heat loss or gain.

2. Control surface temperatures for personnel protection and comfort.

3. Facilitate temperature control of process.

4. Prevent or reduce damage to equipment from exposure to fire or corrosive atmospheres.

5. Reduce emissions of pollutants to the atmosphere.

The temperature ranges within which the term "thermal insulation" will apply, is from -75°C to 815°C. All applications below -75°C are termed "cryogenic", and those above 815°C are termed "refractory".

CHAPTER THREE

3 MATERIALS AND METHODS

3.1 Materials and instruments

Materials used to construct the experimental setup were selected based on local availability and cost effectiveness. The main materials include;

- Aluminum foil
- Aluminum sheet
- Satellite dish
- Copper pipe
- Welding electrode
- Stainless steel sheet
- Glass wool
- Wood ash
- Solar salt

- Elbow
- Wood ash
- Clay pan
- Pump
- Adhesive (mastish)
- Gate valve
- Galvanized steel pipe
- Thermal oil
- Epoxy

Instruments

Thermocouples: were used to record the temperature variations in the heating and storage tank, baking pan inlet, baking pan outlet, surface of the baking pan and ambient temperature.

Infrared thermometer: This was used to measure fluid ad surface temperature

Pyranometer: was used to measure the solar irradiance values

3.2 Conceptual layout
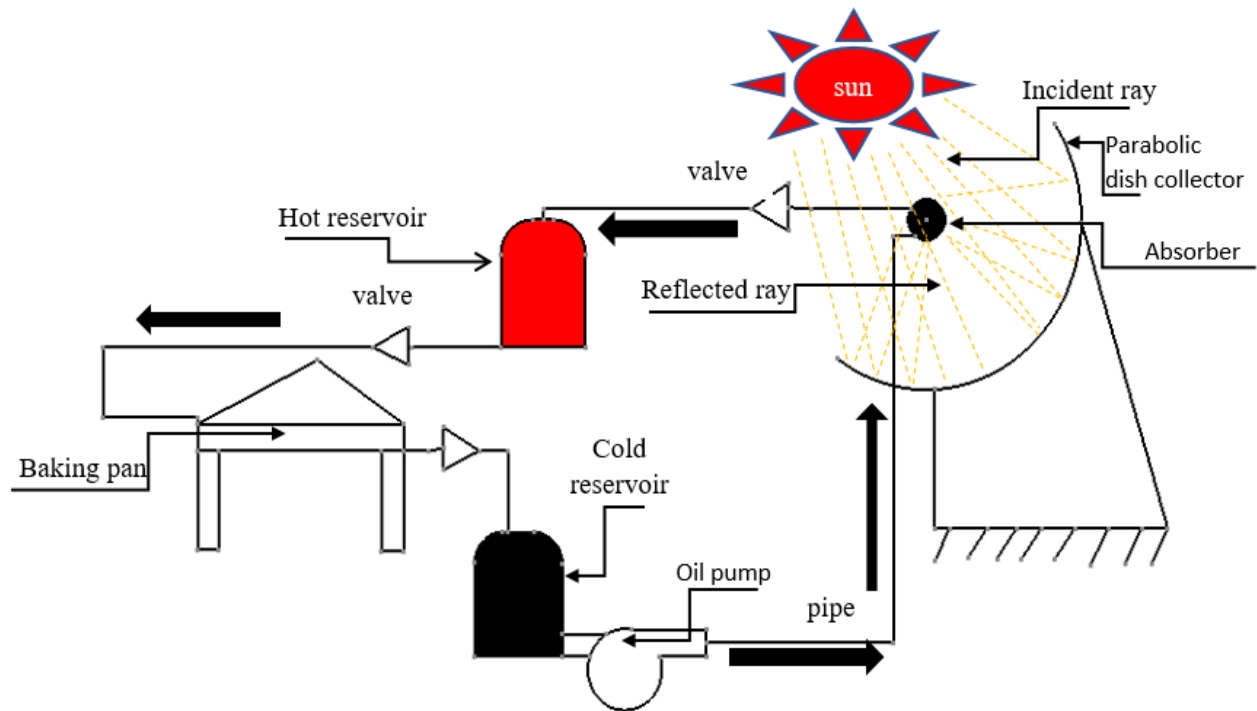
Figure 3.1 Conceptual design of system
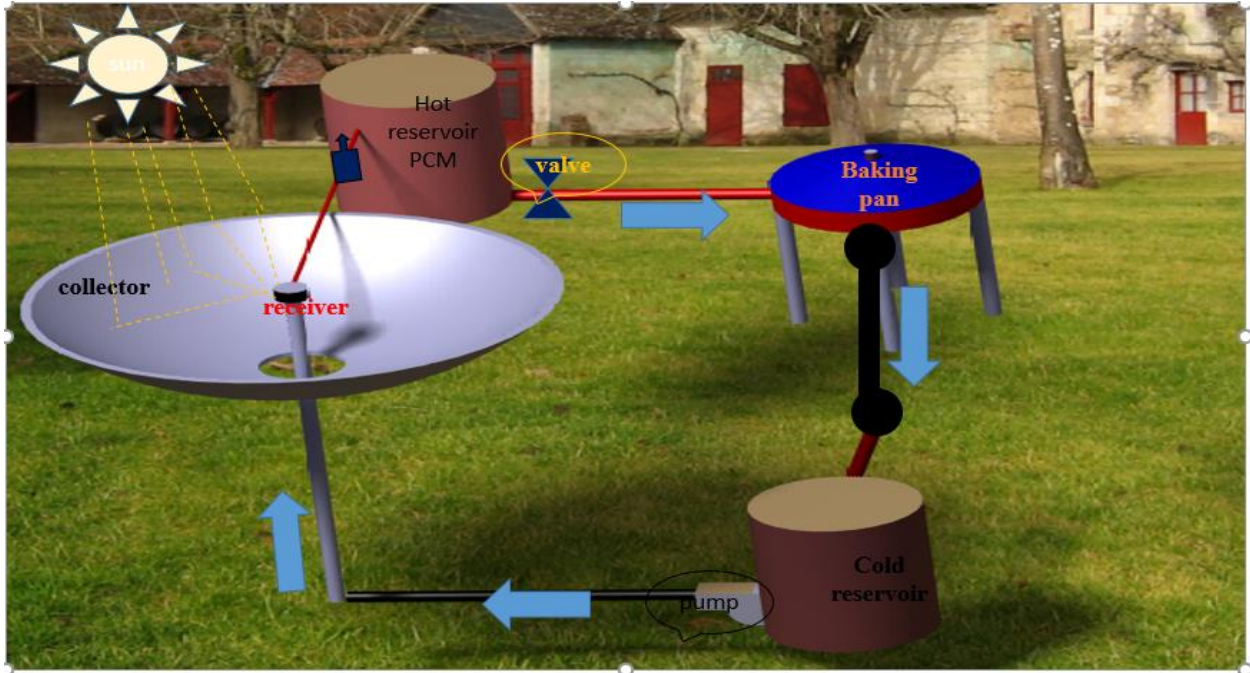
Table 3.1 Solar powered injera baker drawn by Catia software

3.3 Components

The main components of solar powered parabolic dish injera baker are:

1. **pan:** is a flat plate used to bake injera which has a good thermal property to reduce temperature lose during baking to increase the overall efficiency of the system

2. **Parabolic dish type solar collector:** is special kind of heat exchangers that transform solar radiation energy to internal energy of the transport medium. This is a device which absorbs the incoming solar radiation, converts it into heat, and transfers this heat to a fluid (usually air, water, or oil) flowing through the collector. The solar energy thus collected is carried from the circulating fluid in the receiver and flow to a thermal energy storage tank from which can be drawn for use at night and/or cloudy days.

3. **Working fluid:** is a circulating fluid which transporting heat from collector to thermal storage and pan.

4. **Angle iron:** this is used for carrying the pan and the reservoir. Which carry the reservoir and pan at the required level suitable for operation.

5. **Reservoirs:** there are two reservoirs used to store the hot and cold fluid. Hot reservoir stores the fluid after heat by the solar absorber whereas the cold reservoir stores the fluid after discharging the pan. Both reservoirs used for heating and baking processes.

6. **Absorber:** This was made up of black painted spiral copper coil, which absorbs the solar radiation. The black paint enhances the absorptivity of the spiral coil. A good absorber is needed to raise the temperature of the collector.

7. **Insulation:** This prevent the loss of thermal energy at the bottom and on the sides of the collector hence minimize overall heat loss from the system. It is placed above the absorber plate. The insulator must be able to withstand stagnation temperature. Insulating materials

are fiberglass and wood ash. Insulation material selected ensures superior performance with minimum heat loss.

8. **Pump:** which ensure the continuous flow of the fluid through the system. This work uses a single pump only in cold reservoir to avoid high amount of heat lose at the hot reservoir

9. **Thermal storage:** a device which preserve heat for a period of time to bake Injera at night time and cloudy day. Also use to store energy on the day not bake

3.4 Methods

This thesis includes money task on modeling and experimental testing of solar powered Injera baking. Specially it concerns on improving on solar collector and absorbers, selecting on working fluid, improving thermal conductivity of pane by using new composite material to reduce the thermal lose on the pan and reduce thermal lose on pipe.

The above task was accomplished by the following approaches

- By studying different source like books, scientific journal relating to solar collector, pan, thermal storage material and high heat transfer fluid.

- Collection data from Ethiopian meteorology institute to around Bahir Dar

- Modeling finite difference analysis of the pan

- Prototyping and manufacturing of solar injera baker

- Some experimental activity was conducted

Illustration of the research activities of this master's thesis using the engineering model
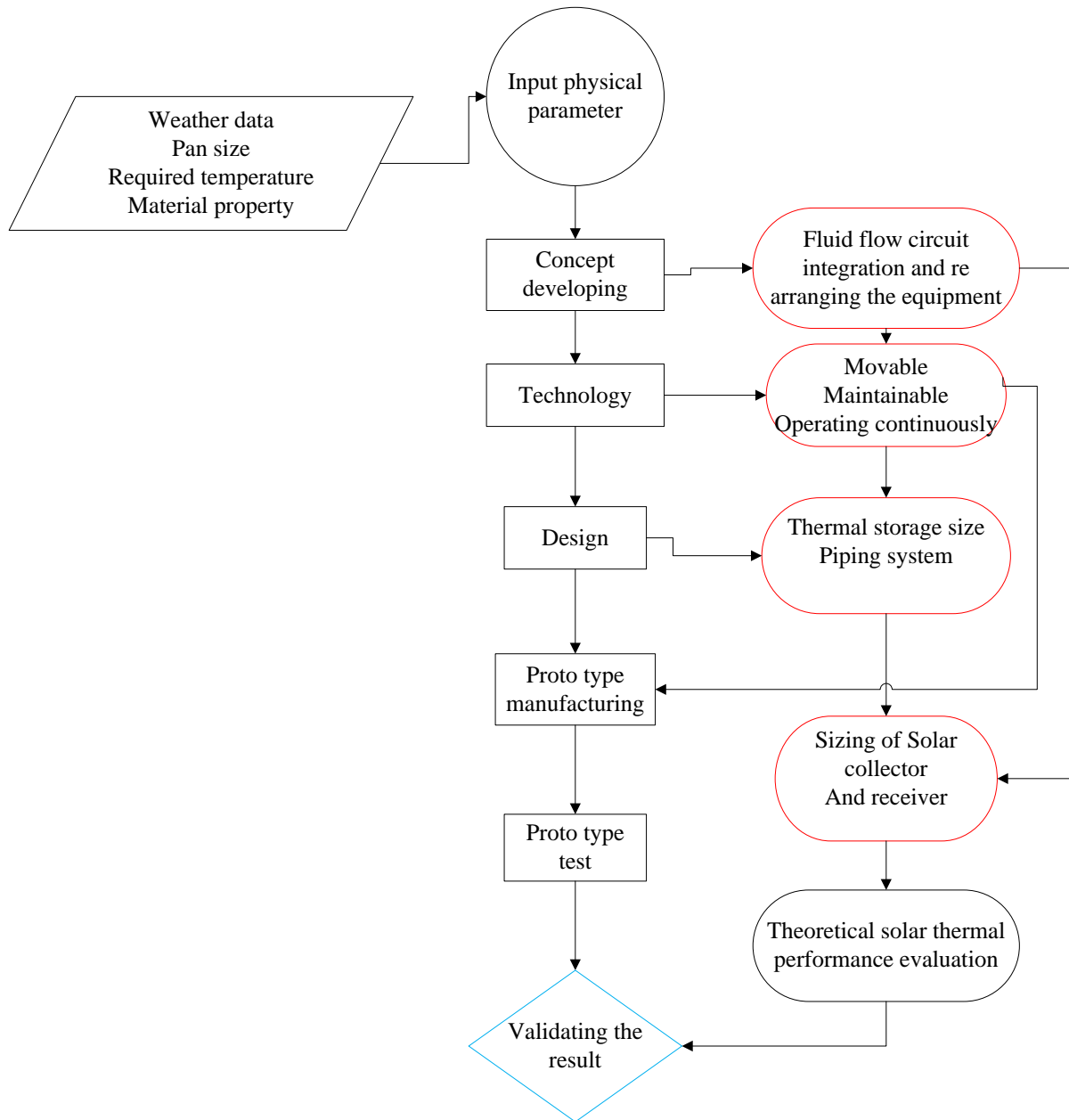
Figure 3.2 Flow chart of research methodology

3.5 Input data

The following section describes the input data that was used to carry out this thesis. This project is conducted for the area Bahir Dar city and around the Bahir Dar and the area have the climatic conditions. And the location is suitable to run the project because of two reasons those are, Bahir

Dar area receives sufficient amount of sun radiation and easy to access the data. The study is on private house. And six persons live there.

To bake 40 Injera per two day

The required temperature to bake Injera is 220℃

The atmospheric temperate of Bahir Dar is 25℃

3.5.1 Daily sunshine hours and radiation of Bahir Dar

From the meteorological data of Bahir Dar, the following data are obtained

Table 3.2Mean monthly sunshine hour

Month	Jan	February	March	April	May	Jun	July	Aug	Sep	Octo	Nov	Dec
SUNHRS	10	10	9	9	8	7	6	6	7	8	9	10

To be clear for design purpose the sun shine hour is put in the range of time

DAILY SUNSHINE HOURE

10h 25%
8-9h 42%
6-7h 33%
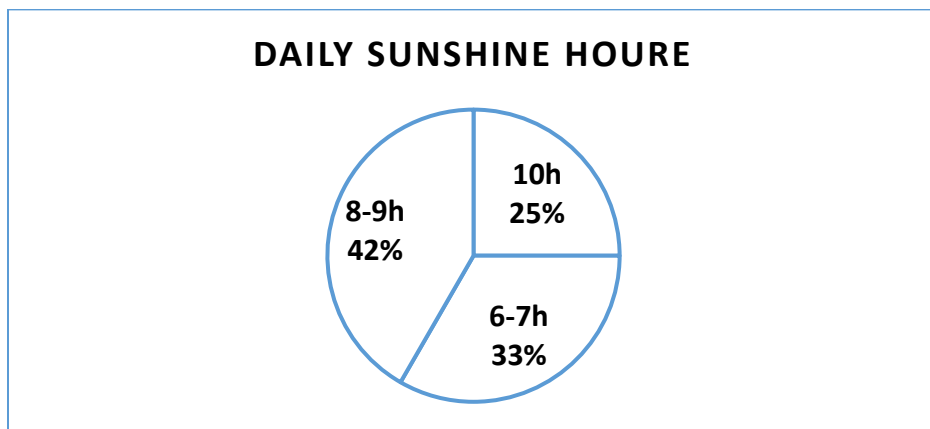
3.5.2 Wind speed and solar intensity

Bahir Dar is located 11.56° in north and 37.37° in east based on this location there is data for Bahir Dar concerning solar energy intensity and wind, the data is taken from NASA

Latitude, °N   +11.56

Longitude, °E   +37.37

Altitude, m   1800

Insolation, kwh/m^2/day   5.76-6.2

Temperature,℃   21.1-22.43

Wind speed, m/s   4.14-4.28

3.6   Thermal analysis solar thermal Injera baker

The solar thermal Injera baking system uses solar radiation as the source of energy. It uses parabolic dish solar collector to convert the solar radiation in to heat energy. The heat energy is conveyed from the source (collector) to the end use compartment (baking pan surface) using heat transfer fluid. The solar powered Injera baking and cooker oven has the following main components:

- The parabolic dish solar collector with its tracking mechanism (to collect and reflect the solar radiation and heat up the heat transfer fluid in the receiver tube).

- Highly insulated thermal storage tank.

- The baking pan assembly (for baking Injera using the heat gained from solar system)

3.7   Energy Required for Injera Baking pan

Baking Injera requires intensive energy and this energy can be defined as the energy necessary to raise the batter to a particular temperature, and evaporate the amount of water that is to be lost during the baking process. To measure the energy utilized in baking Injera, the initial mass of batter, and the total amount of Injera produced from this batter were measured. Thus, the mass of water vapor can be obtained by reducing the mass of Injera produced from the initial mass of batter. It is assumed that the energy utilized to bake the Injera is the energy required in raising the temperature of the batter from room temperature to the boiling point of water which is called sensible heat, plus the energy required to evaporate water which is called latent heat. It is also

assumed that the heat capacity of Injera batter is the same as that of water in order to calculate the energy required to raise the batter temperature to boiling point[2].

Therefore, the utilized energy is

$$E_{utilized} = m_{batter} \times C_P water \times (T_{boil} - T_{room}) + (m_{batter} - m_{Injera}) \times h_{vaporization}$$

Where:

m_{batter}- The mass of the batter expected for one injera= 400g

T_{boil}-the boiling temperature of water $= 94°C$

T_{room} $-$ the room temperature in the baking pan room, $\cong$ 25°C

C_P $-$ the heat capacity of water $= 4.187kJ/kg.k$

m_{Injera} $-$ the mass of the Injera produced $= 320g$

$h_{vaporization}$ $-$ the heat of vaporization of water

$h_{fg} = 2260kJ/kg$

$E_{utilized} = \mathbf{306.41KJ}$

During the baking process there are losses in pipes and in storage tank, so considering the losses and assuming a safety factor of 1.5 the total energy required will be

$$E_{utilized} = 306.41kJ \ x \ 1.5 = \mathbf{459.615kJ}.$$

Total heat required for 40 Injera baking is:$Ereq = \mathbf{18.385MJ}$

The time taken for cooking of one Injera is assumed to be about 2 to 3 minutes taking the 3minutes the power required for Injera baking can be calculated as

$$P = \frac{E_{req}}{t} \qquad\qquad\qquad 3.1$$

Where: P- the power required for baking one Injera $\Delta t = 3 \times 60 = 180$ seconnds

Then, $P = \mathbf{2.553kw}$

The Amount of heat required for heating up a backing Mitad (5mm thick and 50cm diameter) to a temperature of 220℃;

$$Q = m_{pan} \times C_P \times (T_2 - T_1) \qquad\qquad 3.2$$

Where:

C_P −Specific heat capacity of clay = 1.381KJ/Kg℃

T_1 −Initial temperature = 20° C

T_2 −Final temperature = 200° C

$\rho - density\ of\ clay$ =1460 kg/m^3m9

Mass of clay pan (mitad),

$m = \rho \times V$, $V = A \times t = \pi r^2 t = 9.82 \times 10^{-4} m^3$

$m = \rho \times V = 1.4335 kg \approx 1.5 kg$

The amount of energy required to heat the pan, $\boldsymbol{Q = m_{pan} \times C_P \times (T_2 - T_1)}$, which is **365.62KJ**

The time taken to heat the baking pan is in the range of 10-15minutes and possible to take 10minutes. So, the power required to heat baking pan can be calculated as:

$$P = \frac{Q}{\Delta t} \qquad\qquad 3.3$$

Where:

$P\ is\ the\ power\ required\ to\ heat\ the\ pan\ to$ 200℃

$\Delta t\ is\ time\ required\ to\ heat\ the\ pan = 10 \times\ 60s = 600s$

$$P = \frac{365.62KJ}{600s} = \mathbf{609.4watt}$$

Total heat required to bake 40 Injera per two days is 18.75MJ

3.8 Size Specification of Baking Pan (Mitad)

A baking pan is a flat and circular pan commonly about 50 to 60cm in diameter and traditionally used over large clay hearths to bake Injera. The baking pan 'Mitad' considered in this case was 5mm thick and 500mm in diameter and because of its reduced thickness, it has high thermal conductivity than the one which is available in the local market. Direct contact of the pan with the hot heat storage salt solution can cause cracking of the baking pan; therefore, the baking pan is separated from the heat transfer fluid by thin sheet metal cover.

3.9 Required Temperature of the Heat Transfer Fluid in the Storage Tank

When a fluid comes in contact with a solid body, heat exchange will occur between the solid and the fluid whenever there is a temperature difference between the two. During heating and cooling of gases and liquids, the fluid streams exchange heat with the solid surfaces by convection. Energy transfer from heat transfer fluid to the baking pan was in the following two ways

- ➢ Free convection from hot working fluid to pan:
- ➢ Conduction from pan supporting plate to the baking pan: it is the way that in this design analysis in order to protect the pan from cracking when it directly contacts with the working fluid.

Assumptions for the analysis:

- Steady state conditions
- Negligible contact resistance between the supporting plate and pan
- One dimensional heat flow through the y- direction and the pan surface temperature is assumed to be 200℃ (the average)
- The heat storage gallery is well insulated from below and the sides using ash insulation System, and convection and radiation losses are negligible

- Required power to bake one Injera is **2.553KW**
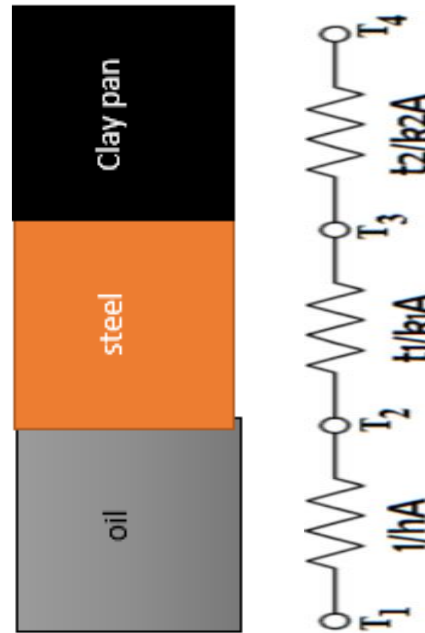
Figure 3.3 Heat Flow

Where:

T1- Hot oil temperature (℃)

T2- Supporting plate lower surface temperature (℃)

T3- Baking pan lower surface temperature (℃)

T4- Baking pan upper surface temperature =200℃

Thus the rate of heat transfers from hot working fluid to baking pan surface can also be expressed as follows[21]

$$Q = \frac{T_1 - T_4}{\frac{1}{hA} + \frac{t_1}{K_1 A} + \frac{t_2}{K_2 A}}$$ *3.4*

Where:

h- Convection heat transfer coefficient thermal oil

t_1- Supporting sheet metal thickness = 0.001m

t_2 - Thickness of baking pan = 0.005m

K_1- Thermal conductivity of supporting plate stainless steel 1%C, K_1= 43w/m. K

K_2- Thermal conductivity of cooking pan = 0.45w/m. K

A- Area of the pan.

Area of the pan is calculated as $A = \frac{\pi D^2}{4}$

Where D is the diameter of the pan= $50cm$

$$A = \frac{\pi \times 0.5^2}{4} = 0.19635m^2$$

Convection Heat Transfer Coefficient: Convection coefficient, h, is the measure of how effectively a fluid transfers heat by convection. To determine the convection heat transfer coefficient first one should determine the Nusselt number and Raleigh number, using Churchill and Chu equations[21]

$$h = \frac{N_u k}{L} \qquad\qquad 3.5$$

$$N_U = 0.27 R_{aL}^{1/4} \qquad\qquad 3.6$$

Where: k- Thermal conductivity

Pr-Pradtel number

Nu - Nusselt number

Ra - Raleigh number

Assuming that the velocity is small and using the formula for free convection; The Raleigh number which is a dimensionless parameter can be calculated from[21]

$$R_a = \frac{g\beta(T_0 - T_\infty)L^3}{\nu\alpha} \qquad\qquad 3.7$$

Where: $\alpha = {k}/{\rho C_p}$ -thermal diffusivity

β —coefficient of thermal expansion

T_0 —operating heat transfer fluid temperature

T_∞ — temperature of the environment= 23.5°C.

l =effective length of the heat transfer surface for ahorizontal circular plate and can be calculated from the relation:

$$l = \frac{A}{P} = \frac{\pi D^2}{4\pi D} = \frac{D}{4} = \frac{0.5}{4} = 0.125m$$

Conduction heat transfer: in the system there is all the three mode of heat transfer taking place. Evaluate conduction heat transfer in the clay pan and plate.

Pan

Made from clay soil with diameter of 500mm and 5mm thickness.
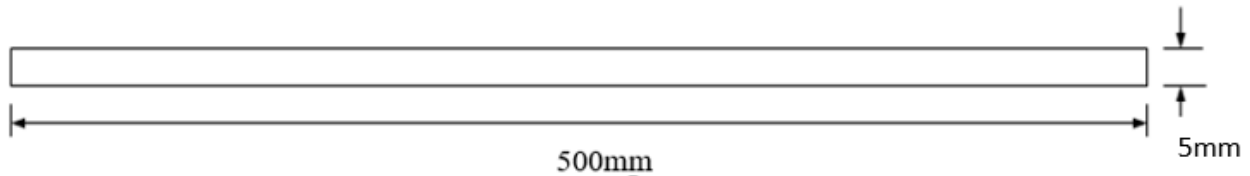
Figure 3.4 Modeling of pan

The upper surface of the pane (T_{usp}) is discuss before which is the temperature required for baking Injera which is $T_{usp} = 200°C$ then the lower surface of the pan (T_{lsp}) is have to be determine by using conduction heat transfer

$$Q = \frac{K_p A (T_{lsp} - T_{usp})}{t_p} \qquad\qquad 3.8$$

Where K_p = thermal conductivity of pan,

$t_p = thickness\ of\ pan,$

$T_{lsp} = T_{usp} + \frac{Q \times t_p}{K_p \times A} = \mathbf{303.33}°C$

Plate

32

Stainless steel with 500m and 1 mm thickness.
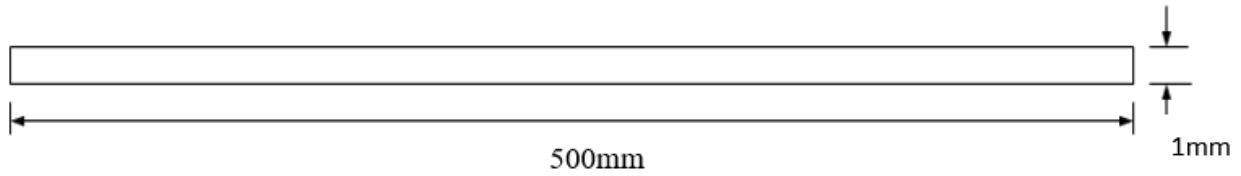
Figure 3.5Modeling of plate

The upper surface temperature (T_{up}) of the plate is the same to the lower surface temperature of the pan calculated in the above which is 303.33°C. And the lower surface temperature T_{lp} of the plate can be calculated as:

$$Q = \frac{K_{plate}A(T_{lp}-T_{up})}{t_{plate}} \qquad 3.9$$

$$T_{lp} = T_{up} + \frac{Q \times t_{plate}}{K_{plate} \times A} = \mathbf{303.6°C}$$

From heat transfer fluid property of Thermia B data from Table 3.2 for initial guess of heat transfer coefficient at the film temperature (T_f).take the temperature of oil $T_{Oil} = 310°C$ and the surface temperature $T_s = 303.6°C$.

$$T_f = \frac{T_{Oil} + T_s}{2} = 306.8°C$$

Using the film temperature at 310°C the property of Thermia B oil can be calculated as:

$$(\rho_\infty - \rho) \approx \rho\beta(T - T_\infty)$$

$$\rho = \frac{\rho_\infty}{1+\beta(T-T_\infty)} \qquad 3.10$$

From equation (), density of the oil is 701.92

The dynamic viscosity, μ of the heat transfer fluid can be calculated as

$$\mu = \frac{k}{C_p}P_r = \rho \times \upsilon \qquad 3.11$$

The thermal properties of Thermia B oil at temperature of 307.13℃ can be get in from property

Table of the oil in Table 3.3 by interpolating between 300℃ and 340℃.[14]

Table 3.3 Property of Thermal oil

Temperature ℃	300	307.13	340
Density kg/m^3	681	676.365	655
Specific heat capacity $KJ/kg\ K$	2.902	3.035	3.648
Thermal conductivity $W/m\ K$	0.114	0.1135	0.111
Prandtl No	11	10.644	9

Since the dynamic viscosity, $\mu = 3.98 \times 10^{-4} pas$

Kinematics' viscosity, $\nu = \frac{\mu}{\rho} = 5.671 \times 10^{-7} \ m^2/s$

Thermal diffusivity (α), $\alpha = \frac{k}{\rho C_p} = 5.33 \times 10^{-8} \ m^2/s$

Then substitute the oil property value in the Rayleigh number (R_{aL})

$$R_{aL} = \frac{g\beta(T_0 - T_\infty)L^3}{\nu\alpha} = 2.92 \times 10^9$$

$$N_{uL} = 0.27 R_{aL}^{1/4} \qquad 10^7 \leq R_{aL} \leq 10^{11}$$

$$N_{uL} = 0.27 \times (2.92 \times 10^9)^{1/4} = 62.748$$

Thus, the average convection heat transfer coefficient can be calculated as;

$$h = \frac{N_{uL}K}{l} = 56.975 \ ^W/m^2.k$$

Now the required oil temperature can be calculated as:

The heat transfer to the plate is equivalent to the heat delivered by the oil and neglect the heat lose through the plate

Thus, $hA(T_{oil} - T_{lsp}) = \frac{-KA(T_{lsp}-T_{usp})}{t_p}$

$$T_{oil} = T_{lsp} - \frac{K(T_{lsp} - T_{usp})}{h.t_p} = \mathbf{305°C}$$

Then, the temperature of the oil is about **305°C**

Then, the amount of energy that has to be stored in the cavity will be

$$E = mC_pT_{oil} \qquad\qquad 3.12$$

The amount of energy required to bake one Injera is calculated in the above is **473.17kJ**

The amount of energy stored in the oil cavity can be calculated by summating the energy in the thermal circuit as:

$$E = E_{Injera} + E_{pan} + E_{plate}$$

$$E = 473.17kJ + m_{plat}C_{plate}(T_{lp} - T_{up}) + m_{pan}C_{pan}(T_{lsp} - T_{usp})$$

$$E = \mathbf{585.3kJ}$$

Then, amount of oil has to be in the cavity can be calculated as:

$$m_{oil} = \frac{E}{C_pT_{oil}} = 0.334kg$$

The volume of the cavity will be

$$V = \frac{m_{oil}}{\rho_{oil}} = \mathbf{4.94 \times 10^{-4}m^3}$$

Design of cold oil storage tanker: a cold oil tank is a single cylindrical structure which have a size of

$$V = \frac{Q_{tatal}}{C_p \times T \times \rho_{oil,220°C}} = \mathbf{12.86 \times 10^{-3}m^3}$$

Pressure in cold oil storage tank; at a full capacity is given

$$P = \rho g H_t \hspace{10cm} 3.13$$

Where $\boldsymbol{\rho}$-density of oil at 200°C is $746 \frac{kg}{m^3}$

g-force to gravity

$\boldsymbol{H_t}$-assuming 1m from delivery side

Then, the pressure of the cold oil is $\boldsymbol{7.318kpa}$

Design of hot oil storage: a hot oil tank is a single cylindrical structure which has a total size of the sum of the amount of oil needed to bake injera for one round.
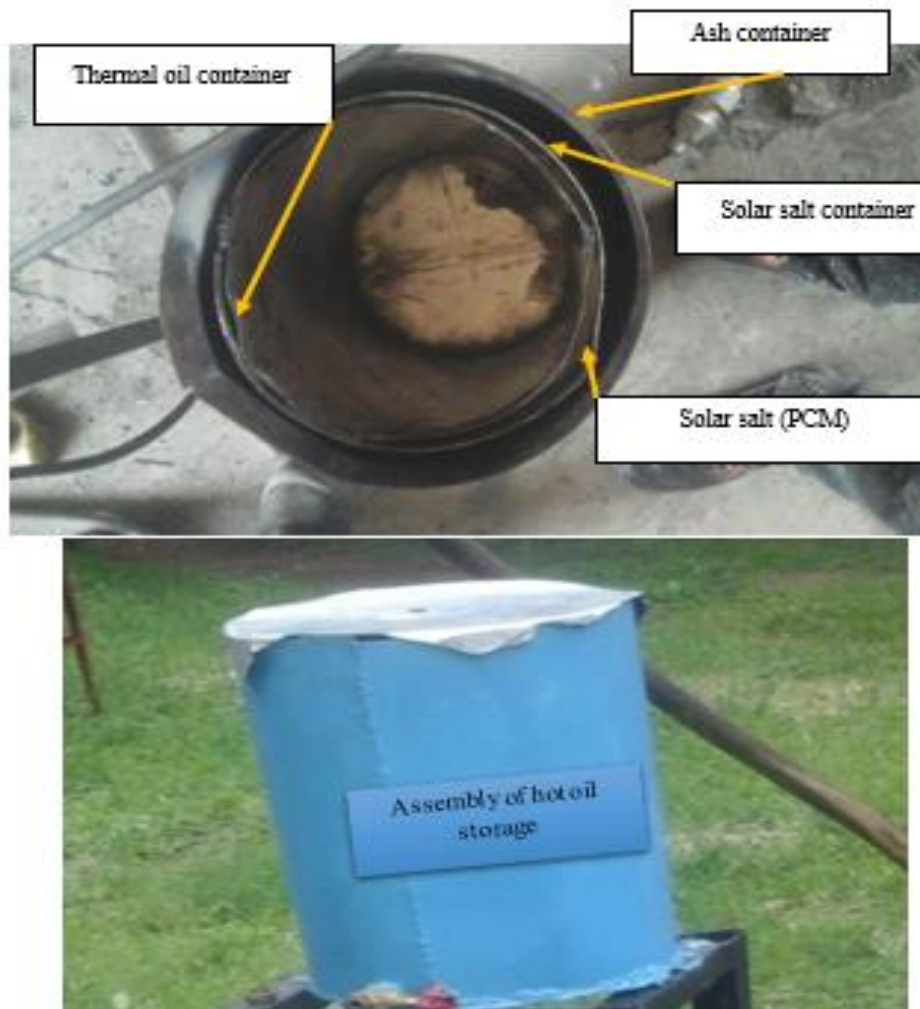
Figure 3.6 Hot oil storage system

The amount of oil has been in hot oil tank can be calculated as

$$V = \frac{Q_{tatal}}{C_p \times T \times \rho_{oil,310°C}} = \mathbf{16.2 \times 10^{-3} m^3}$$

Pressure in hot oil storage tank; at a full capacity is given by;

$$P = \rho g H_t \hspace{5cm} 3.14$$

Where $\boldsymbol{\rho}$-density of oil at 310°C is $674.5 \frac{kg}{m^3}$

g-force to gravity

H_t-assuming 1m from delivery sin

The hot oil pressure in the hot oil storage tank is $\mathbf{6.62 kpa}$

Table 3.4 Parameters of pan and storage materials

Item	Materials	Parameter	Value	Unit
Pan	Clay	Diameter, d_p	0.5	m
		Thickness, t_c	0.005	m
Cavity under pane	Stainless steel	Thickness, t_p	1&3	mm
		Diameter, d_p	0.5	m
Cold storage	Stainless steel	Volume, V_c	12.68	$Litters$
Hot storage	Stainless steel	Volume, V_h	16	$Litters$

3.10 Sizing Thermal storage

Storage material selection

The main important properties of thermal storage container material include;

- Excellent corrosion resistance at high temperature

- A high degree of chemical compatibility between the container material and PCM salt

- Good mechanical properties like strength, creep and thermal fatigue resistance

For solar salt (60wt%NaNO₃/40wt%KNO₃) PCM storage corrosion resistance of stainless steels is better than that of carbon steels and other metals. Since, Stainless steel is an alloy of iron carbon and chromium, as it exposed to solar salt, chromium oxide layer is formed on the surface of the tank wall which prevents the material from corrosion. The small pits observed in the material is due to the rupture in this passive layer. Due to this passive layer the propagation of corrosion through formation of pits is minimum for stainless steel compared to other metals [30]. Due to this reason, stainless steel is used as PCM storage tank material for long-term utilization solar energy. The compatibility of storage tank material depends on corrosion rate of metals as presented in the Table 3.4.

Table 3.5 *Properties of material*

Material	Melting point (℃)	Rate of corrosion ($mg/cm^2.yr$)
Stainless steel	1400-1455	0.3004
Aluminum	660.4	0.9423
Copper	1085	10.9869

The intermittent nature of solar energy needs thermal energy storage systems for baking Injera in door and non-sunny days. In this section, the overall design of solar thermal storage system to bake Injera for one baking session of average family size starting from the selection of material for storage medium, volume, material for tank discussed. The desired properties while selecting a thermal energy storage includes:

- High energy density (per-unit mass or per-unit volume) in the storage material
- Good thermal properties

- Mechanical and chemical stability of storage material

- Compatibility between storage material, HTF and other materials

- Complete reversibility for a large number of charging/discharging cycles or prolonged use

- Minimum thermal Losses

- Ease of control

- Minimal cost.

While, selecting appropriate PCM energy storage for any solar system the phase transition temperature of the material must be near to the operating temperature. The latent heat of phase change should be as high as possible on volumetric basis on order to minimize the size of the storage unit. A high specific heat is required to provide additional sensible heat storage capacity. Enhanced thermal conductivity is also desired to improve charging and discharging process and to have uniform temperature distribution inside the storage unit.

Thus, among three methods of energy storage discussed above latent heat storage systems are promising technique with low heat losses and attractive prices. The thermal energy storage selected as PCM to store heat was a molten salt with mixture of sodium nitrate and potassium nitrate also called solar salt with percentage of ($NaNO_3$ - KNO_3) 60% -40% respectively. It melts at 223℃ and remains in thermally stable liquid phase at temperatures up to 600℃. In this work to use all storage latent storage is not economical feasible to use it. It is better to use both sensible heat and latent heat thermal storage by typical arrangement.
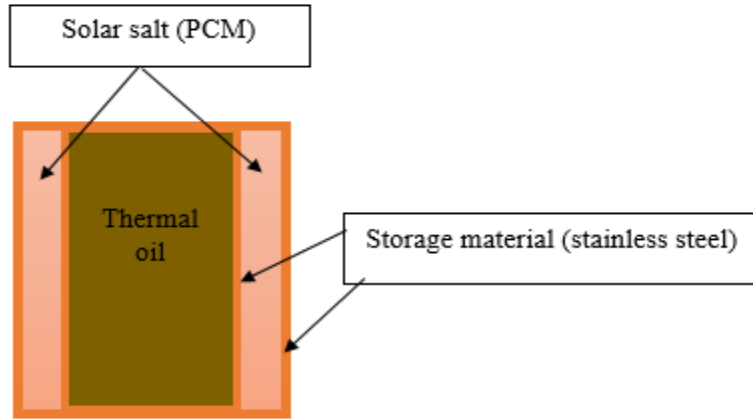
Figure 3.7Hot oil storage tank

For the economic feasibility, it is better to use insulation material for oil container of hot reservoir.

So, to size the thermal storage cover the oil container by solar salt ($NaNO_3$ - KNO_3) 60% -40%

respectively.

Figure 3.8 solar salt (NaNO3 - KNO3)

$$r_{cr} = r_o + \frac{k}{h}$$

<div align="right">3.15</div>

$$r_{cr} = 13cm + \frac{0.4722 \, ^W/_{m°C}}{492.8 \, ^W/_{m^2°C}} = 14cm$$

The thickness of the solar salt have to be 1cm to retain the temperature loss of the thermal oil for a time and this will be insulated with good insulated material.

So, the amount of solar salt (NaNO3 - KNO3) required for this design can be calculated as:

Volume of salt $\quad V = \pi(r_{cr}{}^2 - r_o{}^2) \times h$

Where h is the height of the storage cylinder

The total volume of solar salt is $\mathbf{3.138 \times 10^{-4} m^3}$

3.11 Design of Piping System

This system comprises supply line from cooled oil storage tank to solar collector then from solar collector to thermal storage tank and then from thermal storage tanker to baking pan, after performing the required activity to return the cooled oil to cold oil storage tank. To protect heat loss from the pipes, the piping system was insulated using fiber glass insulation material.

For solar salt (60wt%NaNO3/40wt%KNO3) PCM storage corrosion resistance of stainless steels is better than that of carbon steels and other metals. Since, Stainless steel is an alloy of iron carbon and chromium, as it exposed to solar salt, chromium oxide layer is formed on the surface of the tank wall which prevents the material from corrosion. The small pits observed in the material is due to the rupture in this passive layer. Due to this passive layer the propagation of corrosion through formation of pits is minimum in stainless steel compared to other metals [30].

Material selection

Selection of materials for piping applications is a process that requires consideration of material characteristics appropriate for the required service. Selected material must be suitable for the flow medium and the given operating conditions of temperature and pressure safely during the intended design life of the product.

41

Galvanized steel is the best recommended material for both cold and hot fluid flow because:

- More resistance to corrosion.

- Less thermal conductivity.

- More rigid.

- Cost effective.

- It does not melt due to high temperature steam

Hot fluid pipe design

Hot fluid pipe is used to transfer hot fluid (Thermia B oil) from collector to heat storage tanker and from storage tanker to baking pan. Hot oil pipe sizes will ensure adequate flow rates at appliances and avoid problems

- Oversized Pipe

  - Additional & unnecessary installation costs

  - Delays in obtaining hot salt solution at outlets

  - Increased heat losses from hot fluid pipe

- Undersized Pipe

  - Inadequate delivery from outlets

  - Variation and fluctuation in temperature & pressure at outlets

  - Increase in noise levels

Design of a pipe involves the determination of inside diameter of the pipe and its wall thickness as follows below:

a. **Inside diameter of hot fluid pipe**; the inside diameter of the pipe depends upon the flow rate of hot oil

$$Q = A \times v, Q = \frac{V}{t} = 4.12 \times 10^{-3} litter/sec$$

Where:

v-velocity of the fluid flow

A-cross-section area of the pipe in which fluid flow

Q- flow rate of the oil

t-time required to bake single Injera

V-volume of oil in the cavity

The velocity and cross-section can be calculated as:

$$v = \frac{\mu \times R_e}{\rho \times D} \quad and$$

$$A = \frac{\pi D^2}{4}$$

Where:

μ-dynamic viscosity of oil at 305°C=3.882× $10^{-4} psi$

ρ-density oil at 305°C $= 701.92 kg/m^3$

R_e-Reynolds number =2300 for laminar flow

$$Q = \frac{\mu R_e}{\rho D} \times \frac{\pi D^2}{4} \qquad\qquad 3.16$$

$$D = \frac{4Q\rho}{\pi \mu R_e} = \boldsymbol{4.124 mm}$$

b. **Wall thickness of the pipe:** After deciding the inside diameter of the pipe, the thickness

of the wall (t) in order to withstand the internal fluid pressure (p) may be obtained as:

$$t = \frac{PD}{\sigma_t} + C \qquad\qquad 3.17$$

Where, σ_t-allowable stress 40mpa for steel pipes

We find that for steel pipe, C=3mm,

Thus $t = \dfrac{7.318kpa \times 4.124 \times 10^{-3}m}{40mpa} + 3mm \cong 3mm$

Therefore, the outer diameter of the pipe will be $D_o = D + 2t = 10.124mm$

Hot oil Pipe Insulation

The insulation material should be dimensionally and chemically stable at high temperatures, and resistant to weathering and dampness from condensation. In transporting pipe there is an adiabatic section to be properly insulated to act as a heat proof. The insulation is based on the critical radius of insulation. Locally available insulator is fiber glass.
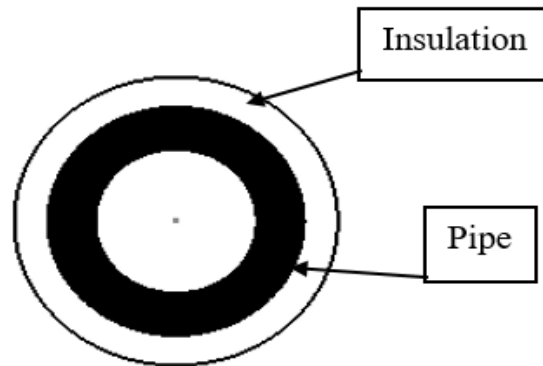
Figure 3.9 Pipe and its Insulation

where: r_o is Pipe outer radius, =5.062mm

r_{cr} is Critical radius of insulation

Thermal conductivity of insulation, k =0.42 w/mk.

Convective heat transfer coefficient of surrounding medium, h =25.4 $^W/_{m^2.k}$

The Critical radius of insulation, r_{cr} for cylindrical body is given by

$r_{cr} = r_o + \dfrac{k}{h} = 7mm$

Flow control valve

Control valve is used to control the flow of heat transfer fluid. Three stainless steel gate valves are used in designing and analysis. The first control valve use to cold fluid that flow from the cold fluid storage tank to the solar collector and it is installed near to the tanker. The second control valve used to control the flow from the receiver to the hot storage tank. This is also installed on the pipe between the receiver and hot storage tank. And allow fluid to flow from receiver to hot storage tank, until required fluid temperature is attained. The last valve also used to control the flow of fluid from hot storage to the pane. All the valve is selected based on the diameter of the pipe.

3.12 Design of parabolic collector (sizing)

3.12.1 THEORETICAL BACKGROUND

Several parameters are used to describe solar concentrating collectors. Given below are brief descriptions of some of these parameters: The aperture area Aa is the area of the collector that intercepts solar radiation. The Acceptance angle is defined as the angle through which a source of light can be moved and still converge at the receiver (Hsieh, 1986). A concentrator with small acceptance angle is required to track the sun continuously while. a concentrator with large acceptance angle needs only seasonal adjustment. The absorber area A_{abs} is the total area of the absorber surface that receives the concentrated solar radiation. It is also the area from where useful energy can be extracted. The Concentration Ratio C is defined as the ratio of the aperture area to the absorber area and can be written as:

$$C = \frac{A_a}{A_{abs}} \hspace{5cm} 3.18$$

The optical efficiency η_o is defined as the ratio of the energy absorbed by the absorber to the energy incident on the concentrator aperture (Garg and Prakash, 2000). It includes the effect of

mirror/lens surface, shape and reflection/transmission losses, tracking accuracy, shading, receiver-cover transmittance, absorbance of the absorber and solar beam incidence effects. The optical efficiency is given as:

$$\eta_o = \frac{P_{abs}}{A_a \times I_D}$$
3.19

The optical efficiency of most solar concentrators lies between 0.6 and 0.7. In a thermal conversion system, a working fluid is used to extract energy from the absorber. The thermal performance of solar concentrator is determined by their thermal efficiency.

The thermal efficiency is defined as the ratio of the useful energy delivered to the energy incident at the concentrator aperture:

$$\eta_{th} = \frac{\rho V c_{pf}(T_2 - T_1)}{I_b \times A_a}$$
3.20

The incident solar radiation consists of beam (direct) and diffuse radiation. However, the majority of concentrating collectors can utilize only beam radiation.
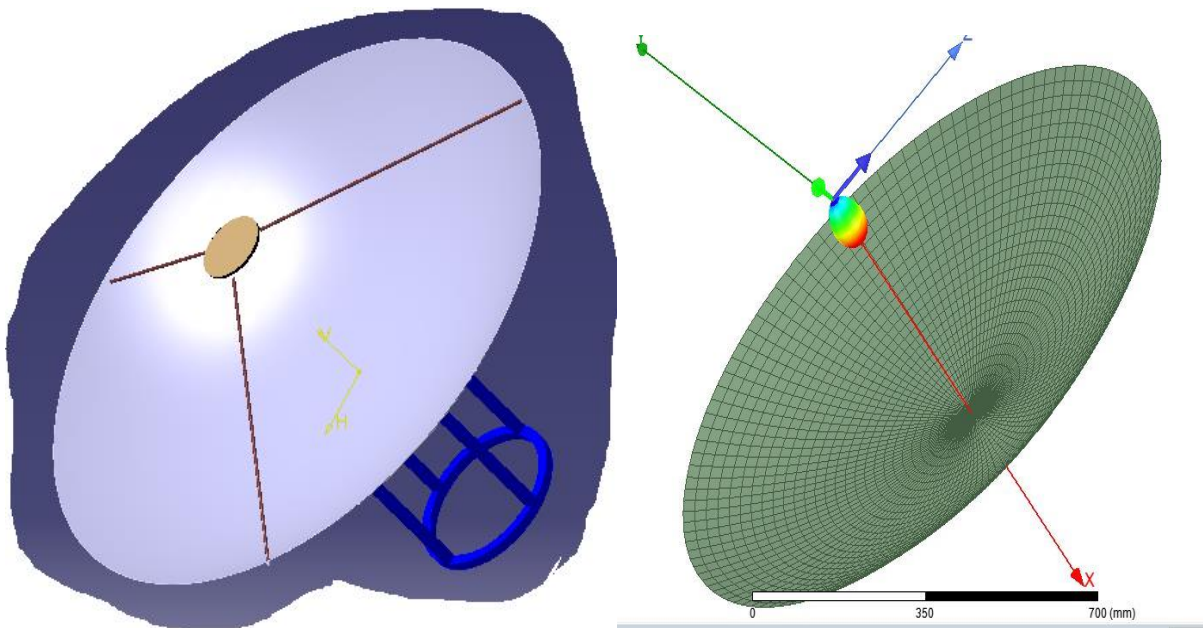
Figure 3.10 Parabolic dish

The instantaneous thermal efficiency of a solar concentrator may be calculated from an energy balance on the absorber. The useful thermal energy delivered by a concentrator is given by:

$$q_u = \eta_o I_b A_a - U_L(T_{abs} - T_a)A_{as}$$ 3.21

Therefore, the instantaneous thermal efficiency may be written as:

$$\eta = \frac{q_u}{I_b A_a} = \eta_o - \frac{U_L(T_{abs} - T_a)}{I_b \cdot C}$$ 3.22

At higher operating temperatures the radiation loss term dominates the convection losses and the energy balance equation may be written as

$$q_u = \eta_o I_b A_a - U_L\left(T_{abs}^4 - T_a^4\right)A_{abs}$$ 3.23

In a parabola, all the incoming solar rays from a light source are reflected back to the focal point of the parabola. The solar concentrator was developed using a semi-spherical surface covered with many small sections of mirrors to form a segmented, spherical concentrator. The frame of the parabola was made from a mini dish satellite receiver plate. The solar concentrator takes advantage of all incoming solar radiation and concentrates it at the focus.

Figure 3.11 shows the parabolic dish concentrator parameters. The equation for the parabola in cylindrical coordinates is given by:

$$Z = \frac{r^2}{4f}$$ *3.24*

The diameter of the opening parabolic surface is d, and the focal distance of the parabola is f. the surface of this parabola is given by:

$$S = \left\{\left[1 + \left(\frac{d}{4f}\right)^2\right]^{\frac{3}{2}} - 1\right\}$$ *3.25*

The cross-section of the opening is:

$$A = \frac{\pi d^2}{4}$$ *3.26*

To calculate the focal distance, the following equation is use

$$f = \frac{d^2}{16h}$$ 3.27
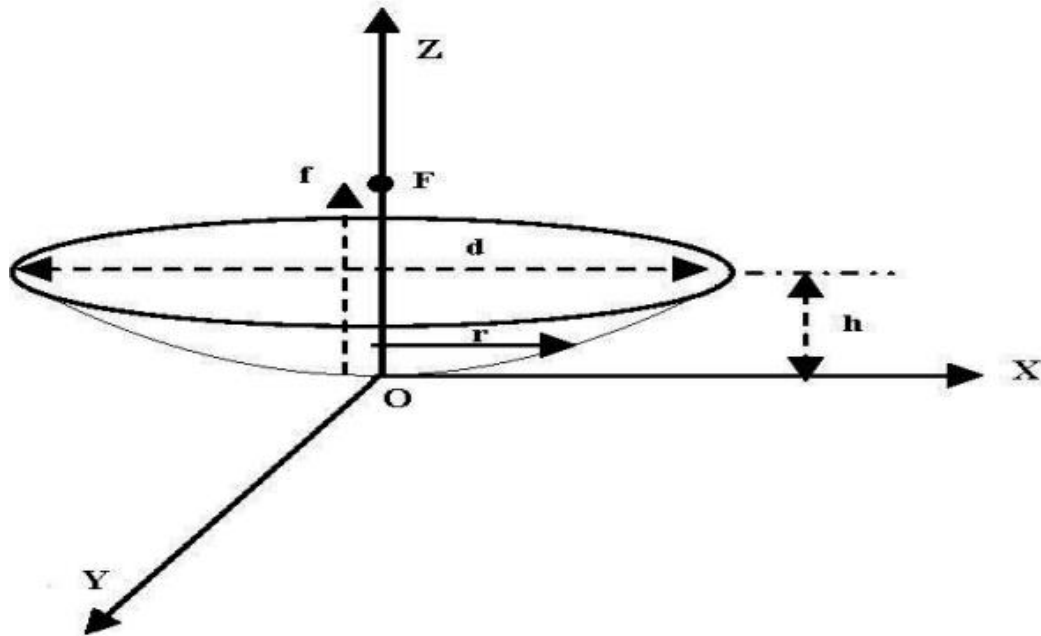
Figure 3.11 parabolic dish concentrator parameters

Where: h is the height of the dish

d is the diameter of the dish

f is the focal point

F is the load

r is the radius

Material selection

Material selection for the reflector of dish is the most essential factors to be considered while designing parabolic dish reflector for any solar thermal system. The reflectivity property of the material of the concentrator highly affects the performance of the collector.

Table 3.6 Properties of typical reflector materials

Material	Reflectivity (ρ)	Cost
Aluminum foil	85%	Relatively low
Glass mirror	96%	Relatively high

As shown in the table glass has high reflectivity but difficult to manufacture to the desired parabolic shape. Due to the cost and ease of fabrication aluminum foil is used as reflector material and aluminum sheet at the back of the reflector.

3.12.2 Sizing of parabolic dish collector

In order to calculate the area of a collector, the total amount of energy required to cook and baking is required as we calculated previously the total amount of energy became, $E_{total} = \mathbf{18.385MJ}$

The total solar radiation exposure around Bahir Dar is from $5.76\ to\ 6.2\ Kwh/m^2/hour$ which have an average solar beam radiation of $\mathbf{5.98\ Kwh/m^2/hour.}$ And the average sunshine hour is

6 hour

Global solar radiation for exposure over $1m^2$ for one hour is $720w/m^2$

The estimated useful energy $q_u = \dfrac{E_{total}}{t_{sun\ shin}} = \mathbf{619w}$

The useful power can be calculated as:

$$\dot{Q}_u = \eta_{th}I_bA_a \qquad\qquad 3.28$$

The efficiency range of most solar concentrators is 40% - 60% (Magal, 1993). Hence for Kaduna (Mohammed, 2009):

Then the aperture area of collector required to achieve the above amount energy become

$$A_a = \frac{q_u}{\eta_{th}I_b} = 2m^2$$

The area of aperture area $A_a = \dfrac{\pi d^2}{4}$,

The diameter of the parabolic dish collector is 1.7m

Spiral coil receiver is selected over cavity receivers due to its simplicity in transporting the oil (fluid) in the collector loop. Spiral coil absorber where HTF oil circulates inside is exposed to the concentrated solar radiation and absorbs the incoming radiation[22].

Table 3.7 Typical design specification of parabolic dish reflector

Parameter	unit	Value
Aperture area, A_a	m^2	2
Aperture diameter, d_a	m	1.7
Focal length	M	0.65
Rim angle	°	60
Dish height, h	m	0.32
Concentration ratio, C	—	50
Beam radiation,I_D	$^W/_{m^2}$	720
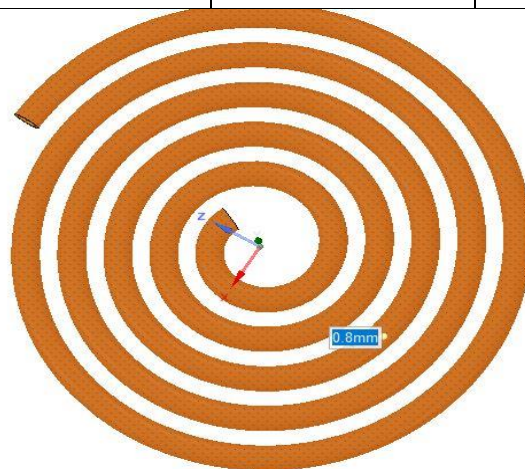
Table 3.8 Spiral coiled receiver

It is better to construct a parabolic dish with a concentration ratio greater than 10 and then it was set to be 50 for this design. Thus, having the aperture area and geometric concentration ratio, receiver area of the dish was calculated from;

$$C = \frac{A_a}{A_r} \qquad\qquad 3.29$$

The receiver diameter determined from the relation of receiver area and this diameter was the maximum outer diameter of the spiral coil;

$$A_r = \frac{\pi Dr^2}{4} \qquad\qquad 3.30$$

It is known that at theoretical focal point the concentration of solar radiation was at a fixed point, thus it is highly recommended to lower the focal distance to avoid local heating due to point concentration. Thus, the actual focal distance (f_actual=0.65m) should be lower than the theoretical which is determined from similarity of triangles or trigonometric relations

Where;
VF-Theoretical focal distance
VP-Actual focal distance   Where: D_a-aprature area
D_r-receiver area
h- Height of dish
V-vertex of dish
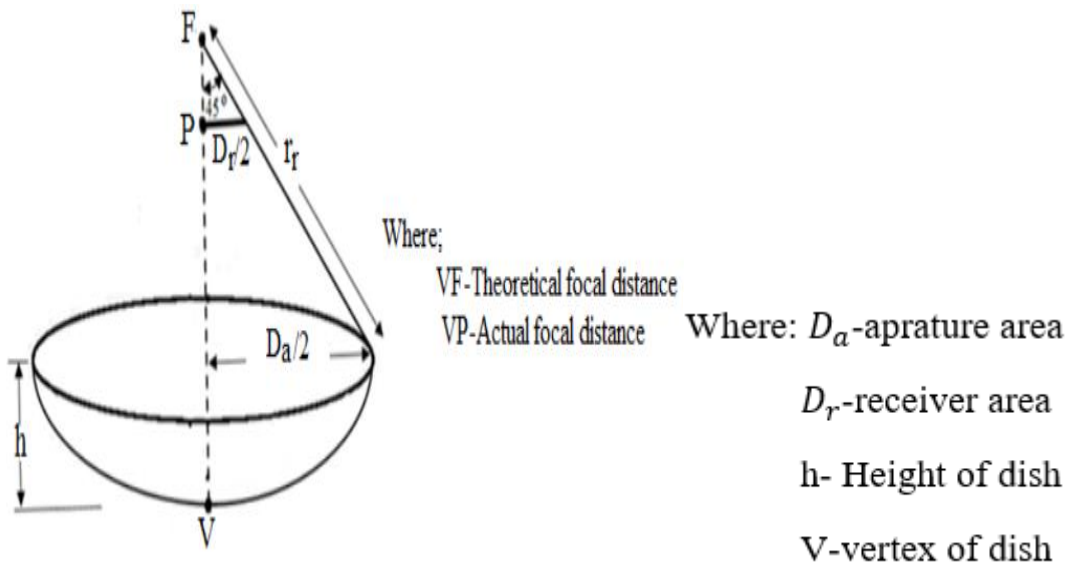
Table 3.9 Locating the actual focal length of the receiver[23]

3.13 Experimental setup and measuring

The experiment setup and measuring instrument is as shown in figure 3.12 and figure3.13. The set up was place in Bahir Dar institute of technology around stadium; the parabolic dish concentrator was set to move freely in any direction by rotating dish manually. And the receiver was set at station connected with hot and cold reservoir by fluid transfer pipe. The focal point of the dish was found by moving the dish free until pointing at the receiver.

Figure 3.12 Instrument use during experiment
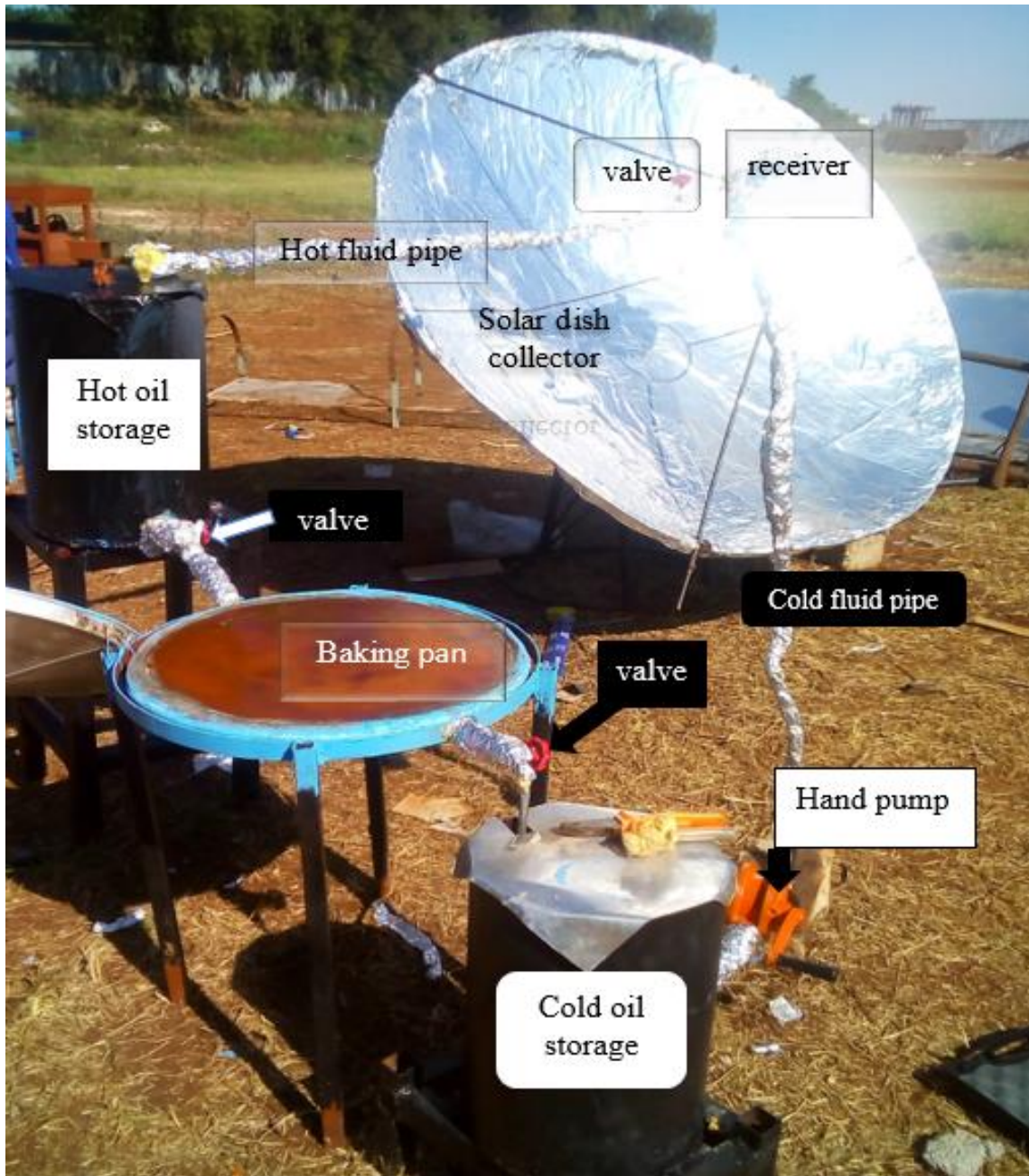
Figure 3.13 Porotype of the all over work

3.14 Performance Evaluation of the system

3.14.1 Optical performance of parabolic dish concentrator

Optical efficiency refers to performance of a collector which depends on the optical properties of the collector materials, the geometry of the collector, and the various imperfections arising from the construction of the collector. It can be characterized by the following optical loss encountered during practical work[67].

- **Reflectivity (ρ):** It is the property of reflector material and defined as the ratio of radiation reflected to the receiver and that of impinging on the reflective surface of the dish. Aluminum foil with reflectivity of 85% was used due to ease of manufacturing and cost for this application

- **Absorbance (α):** it is the property of the receiver material and expressed as fraction of reflected radiation hitting the receiver coil surface is absorbed. Hence, well insulated, isothermal receiver, painted black, and with no transparent glass cover has effective absorptance of one (blackbody).

- **Shading loss (A):** refers to part of the reflective area of the dish shaded by the receiver. Since, the parabolic dish concentrator aperture area is much larger than the receiver area, it is advisable to take minimum which is less than 1% shading loss.

- **Intercept factor (γ):** is termed as the fraction of reflected radiation incident on the receiver/absorber. It is also called spillage loss which defined as a portion of solar radiation reaching outside the receiver aperture and total loss of about 1–3% is considered.

- **Cosine loss:** It is the ratio of total reflective area and its projected area, as seen from the sun. But, the optical axis of parabolic dish collectors is always pointing directly towards

the sun to reflect the beam so that the incidence angle of beam radiation into the dish is zero degree. Thus, the cosine loss becomes zero for this analysis.

Generally, the optical performance of parabolic dish solar concentrator highly affected by the combined effect of the above-mentioned optical losses. In addition, different operational errors such as structural, tracking, alignment and others should also be considered during experimental analysis.

Thus, optical efficiency of parabolic dish concentrator with spiral coil absorber is given by[15], [22]:

$$\eta_o = A\gamma\rho\alpha \qquad\qquad 3.31$$

3.14.2 Useful energy and thermal loss

The thermal model of spiral coiled tube absorber is based on the energy balance between the HTF, absorber/receiver, and surrounding. Here, the energy balance considers the direct/ beam solar radiation falling on the reflector, various optical losses, thermal losses and the useful heat gained by the HTF. Development and implementation of spiral coil heat absorbers for parabolic dish solar collector application is the best alternative due to its compactness and efficient heat transfer capability. Secondary flow occurs during the flow of oil along the curved pipe induced by centrifugal force and it significantly enhances the heat transfer rate[22].

The incoming beam solar radiation is absorbed by the back plate and black coated spiral coiled tube absorber Q_{abs} and optical losses was considered in the heat flux terms. The heat from the receiver tube is carried by the HTF by convection ($Q_{r-f,conv}$). The radiation ($Q_{r-a,rad}$) and convection ($Q_{r-a,conve}$) losses from the receiver tube to the surrounding air and the conduction ($Q_{r-a,cond}$) loss through the receiver back were accounted in this model.
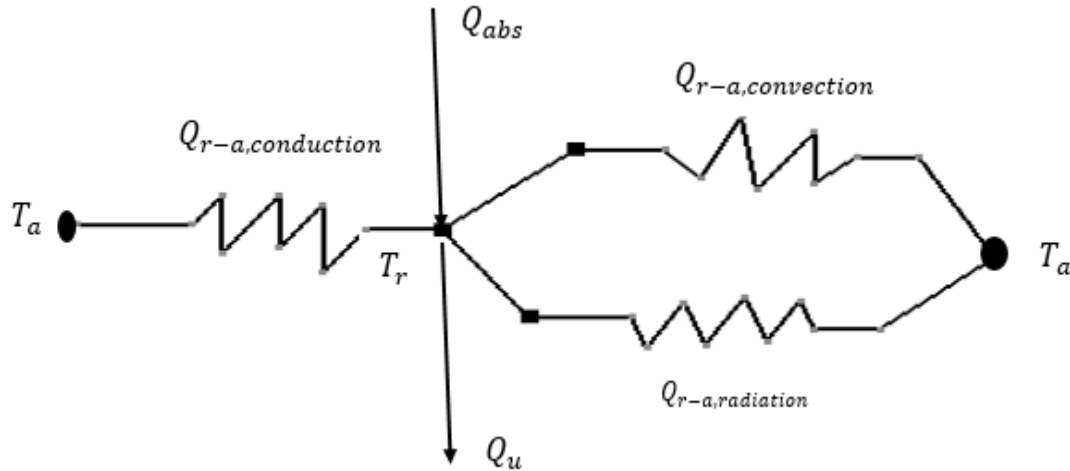
Figure 3.14 Receiver thermal resistance model

From the model the use full energy is the heat transfer to fluid flow inside the receiver by convection can be calculated [2][15][22] :

$$Q_u = Q_{abs} - Q_{loss} \qquad 3.32$$

Where, Q_{loss} is the fraction of energy loses by conduction, convection and radiation. And the absorber heat energy becomes the product of collector optical efficiency and solar irradiance incident on the aperture of the dish aperture.

$$Q_{abs} = \eta_o G_B A_a \qquad 3.33$$

The useful heat gain by the HTF oil is also determined from the convective heat transfer relation[15].

$$Q_u = A_{sc} h (T_r - T_{fm}) \qquad 3.34$$

Where, h is the heat transfer coefficient between the HTF and the receiver coil

A_{sc} the heat transfer area of spiral coil

T_{fm} the fluid mean temperature, $T_{fm} = \frac{T_{out} - T_{in}}{2}$

The critical Reynolds number for flow along spiral coil pipe is higher than that of straight pipes. For spiral coil pipe flow there are two critical Reynolds numbers one is when the fluid enters from the outermost turn and the other is when the fluid enters from the innermost turn. Therefore, for this study the fluid enters from the outermost turn and the corresponding transition Reynolds number is given by:

$$R_{e.cr} = 2300 \left[1 + 4.9 \left(\frac{d_i}{R_{max}} \right)^{0.21} \left(\frac{p}{R_{max}} \right)^{0.1} \right] \qquad 3.35$$

According to the above equation for laminar flow inside the spiral pipe, Reynolds number R_e will be less than 7130 and the corresponding average Nusselt number for the fluid flowing through smooth pipe can be obtained by;

$$N_u = 0.023 R_e^{0.8} Pr^{0.4} \qquad 3.36$$

Hence, the convective heat transfer coefficient between coil absorber pipe and hot oil is obtained as;

$$h = \frac{N_u \times k}{d_i} \qquad 3.37$$

The conduction heat loss from the black plate of the receiver to the ambient via its top insulation was obtained using the relation;

$$Q_{b-r,cond} = \frac{A_r \times K}{t} (T_r - T_a) \qquad 3.38$$

Where, A_r is area of receiver, m^2

K thermal conductivity of thermal insulation, $w/m.k$

t insulation thickness, m

The convective heat loss from the receiver to ambient is given by;

$$Q_{r-a,conv} = A_r h_{air} (T_r - T_a) \qquad 3.39$$

Where, h_{air} heat transfer coefficient of air, $w/m^2.k$

The heat loses by radiation,

$$Q_{r-a,rad} = A_r \varepsilon_r \sigma \left(T_r{}^4 - T_a{}^4 \right) \qquad\qquad 3.40$$

Where, ε_r emissivity of black painted receiver

σ is the Stefan -Boltzmann constant $=5.67 \times 10^{-8} \, w/m^2 k^4$

Note that the ambient temperature is used in radiation heat loss calculation because the spiral coil absorber does not radiate with the sky temperature as it faces to the ground.

Finally, the total rate of heat loss of the absorber becomes

$$Q_{loss} = Q_{b-r,cond,} + Q_{r-a\ conv} + Q_{r-a,rad} \qquad\qquad 3.41$$

3.14.3 Thermal Performance of Parabolic Dish Concentrator

The collector efficiency (collector performance) is the ratio of useful heat gain to that of the incident solar radiation. Useful energy extracted by the fluid is related to the absorbed solar radiation and the total thermal loss of the receiver. The absorbed radiation per unit aperture area can be estimated from the radiation and optical characteristic of solar collector. The thermal losses must be estimated from the summation of radiation, convection and conduction losses of the absorber/receiver. The instantaneous efficiency of a collector can be determined by useful heat gain of the HTF, the total thermal loss of the receiver/absorber and the amount of solar radiation incident on the aperture of the dish. The hourly efficiency of a collector should be considered as instantaneous efficiency and expressed by:

$$\eta_i = \frac{Q_u}{I_B A_a} \qquad\qquad 3.42$$

CHAPTER FOUR

4   RESULTS AND DISCUSSION

Experimental testing where conducted in clear shine sun day during December 5-7/2012 E.C. During the experiment, different thermal equipment where used for measuring the required parameters relevant to this thesis work and to evaluate the performance of the system. Thermo couple, infrared thermo meter is used to measure the atmospheric temperature, receiver temperature, inlet and outlet fluid temperature of receiver and fluid temperature at different point of the system. Solar meter or pyranometer is used to measure the variation of radiation use function of time throughout a day.

4.1   Thermal performance evaluation of the receiver

The performance evaluation of the power block of the system was evaluated for three consecutive day from December 5-7/2012. The reading of data and performance evaluation was started from 2:00-11:00 local time (8:00am-5:00pm) and the data was collected at 1-hour interval.

At the time of evaluating the performance of the power block system, the weather station equipment was showing its prediction sign that the ambient temperature and solar radiation were kept increasing with time changing during starting of the fluid to receiver.

Figure 4.1 shows the plot of ambient temperature (Ta), solar irradiation and time of the day. From the figure it was observed that the highest solar irradiation was obtained $919^W/_{m^2}$ at 8:00 local time. The useful energy was extracted from 2:00 to 11:00 local time as shown below though from 4:00 to 10:00 is best that means around for 6hours a day.

Figure 4.2 shows the plot of receiver temperature, receiver fluid temperature and time of the day. From the figure it was observed the temperature was obtained around the middle of the day which was from 4:00 to 10:00 local time. An efficient time was around six hours in a day at which highest ambient temperature and solar radiation was recorded. As shown in figure 4.1 and figure 4.2 temperature of the receiver and fluid was directly proportion with solar radiation and ambient temperature.
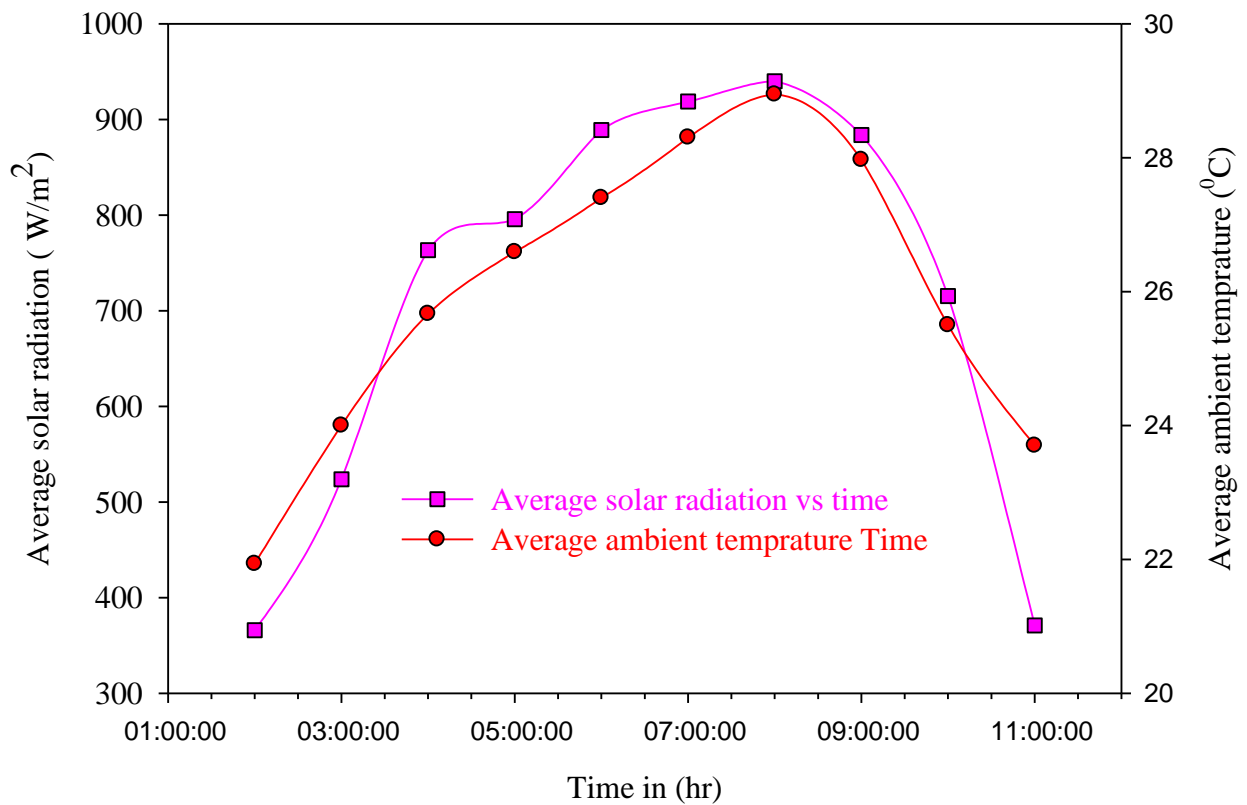
Figure 4.1 Daily Average ambient temperature and solar irradiation with time
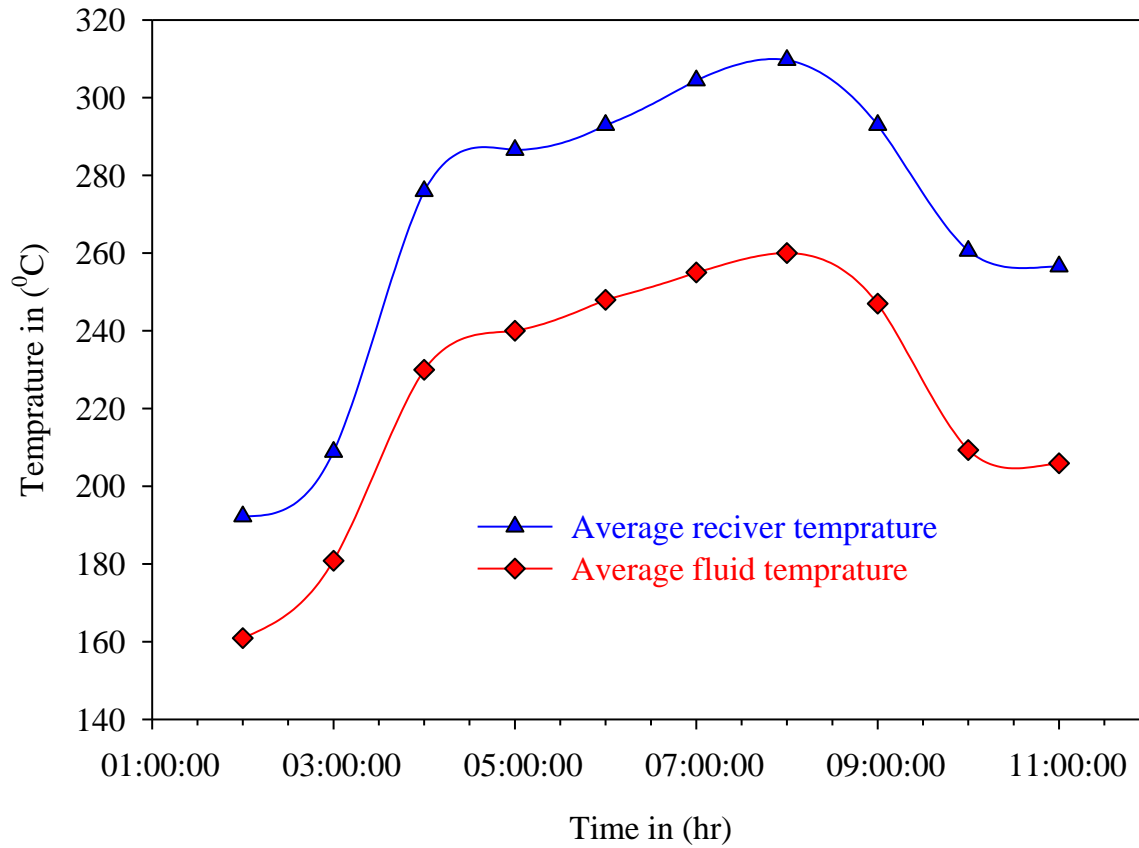
Figure 4.2 Daily Receiver temperature and receiver fluid outlet temperature

The test results indicate that the maximum fluid temperature reached 253℃ at noon time when the maximum solar radiation and ambient temperature were 940W/m2 and 30℃. The daily variation of fluid temperature as a function of time given in the figure 4.3.
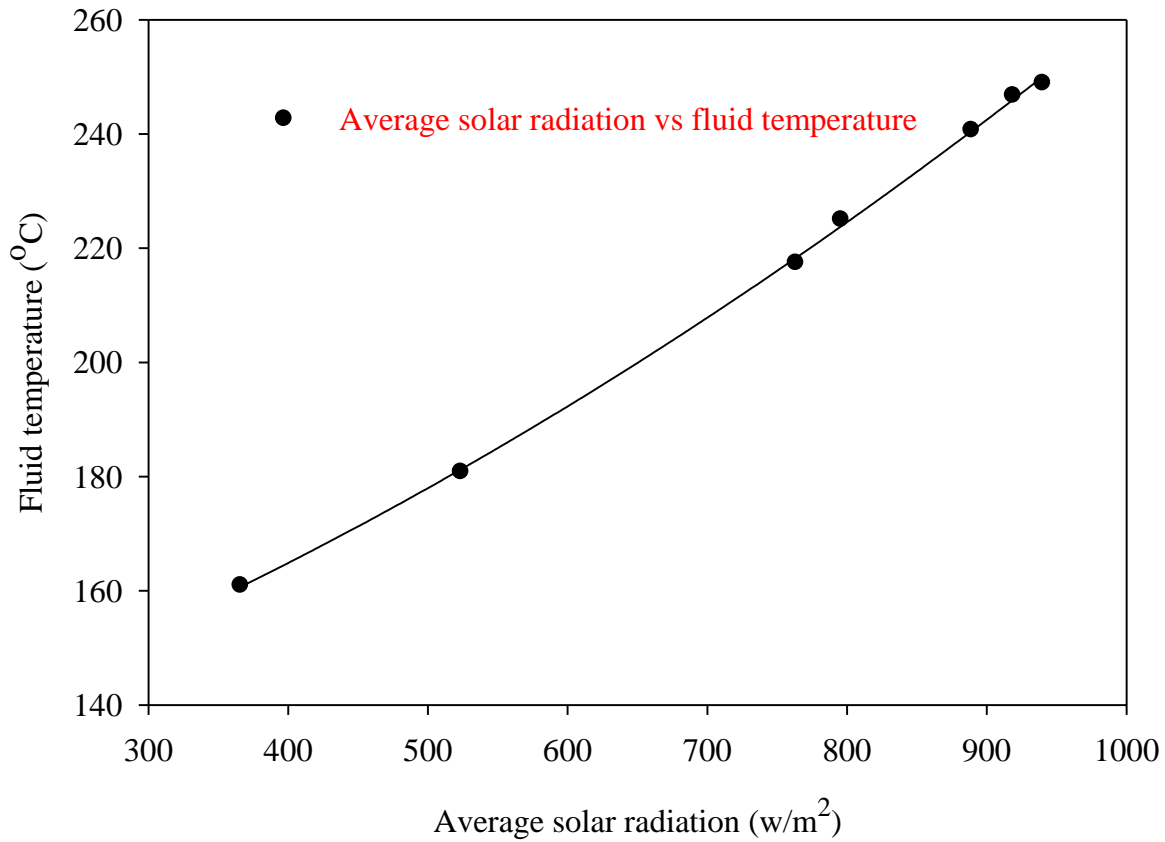
Figure 4.3 Fluid temperature with variation of solar radiation

The performance of a solar thermal system depends on the performance of a solar concentrator. The collector performance parameters such as the absorbed radiation, thermal loss, useful energy and instantaneous efficiency were listed in table 4.1.

Table 4.1 Results for thermal performance parameters of parabolic dish solar collector

Time	$I_B(^W/_{m^2})$	$T_a(°C)$	$\dot{Q}_s(^W/_{m^2})$	$\dot{Q}_{ab}(^W/_{m^2})$	$\dot{Q}_{loss}(^W/_{m^2})$	$\dot{Q}_u(^W/_{m^2})$	η_i
2:00	366	22	732	439.2	173.036	280.896	0.639
3:00	523.67	24	1047.33	628.4	188.691	355.2772	0.565
4:00	763.33	25.7	1526.67	916	262.1056	438.748	0.479
5:00	795.67	26.59	1591.33	954.8	273.713	481.2548	0.505

6:00	889	27.4	1778	1066.8	280.605	491.7884	0.461
7:00	918.67	28.3	1837.33	1102.4	293.695	505.5672	0.460
8:00	940	30	1880	1128	298.445	510.4768	0.453
9:00	883.67	29	1767.33	1060.4	279.009	466.9288	0.441
10:00	715.33	29	1430.667	858.4	244.489	420.2192	0.490
11:00	371	23.7	742	445.2	182.977	290.244	0.651
Average	716.634	26.569	1433.266	859.96	247.6766	424.14	0.5144

It has been seen that from the test result the average daily solar thermal efficiency of this solar concentrator becomes 51.44% which is near to the theoretically designed value and thus, the thermal performance of the collector was satisfactory.

Figure 4.4 shows the thermal efficiency versus the ratio of temperature difference of the inlet and outlet receiver oil temperature to solar radiation intensity. The graph has a negative slope and the optimum thermal efficiency has been at the middle of the day.
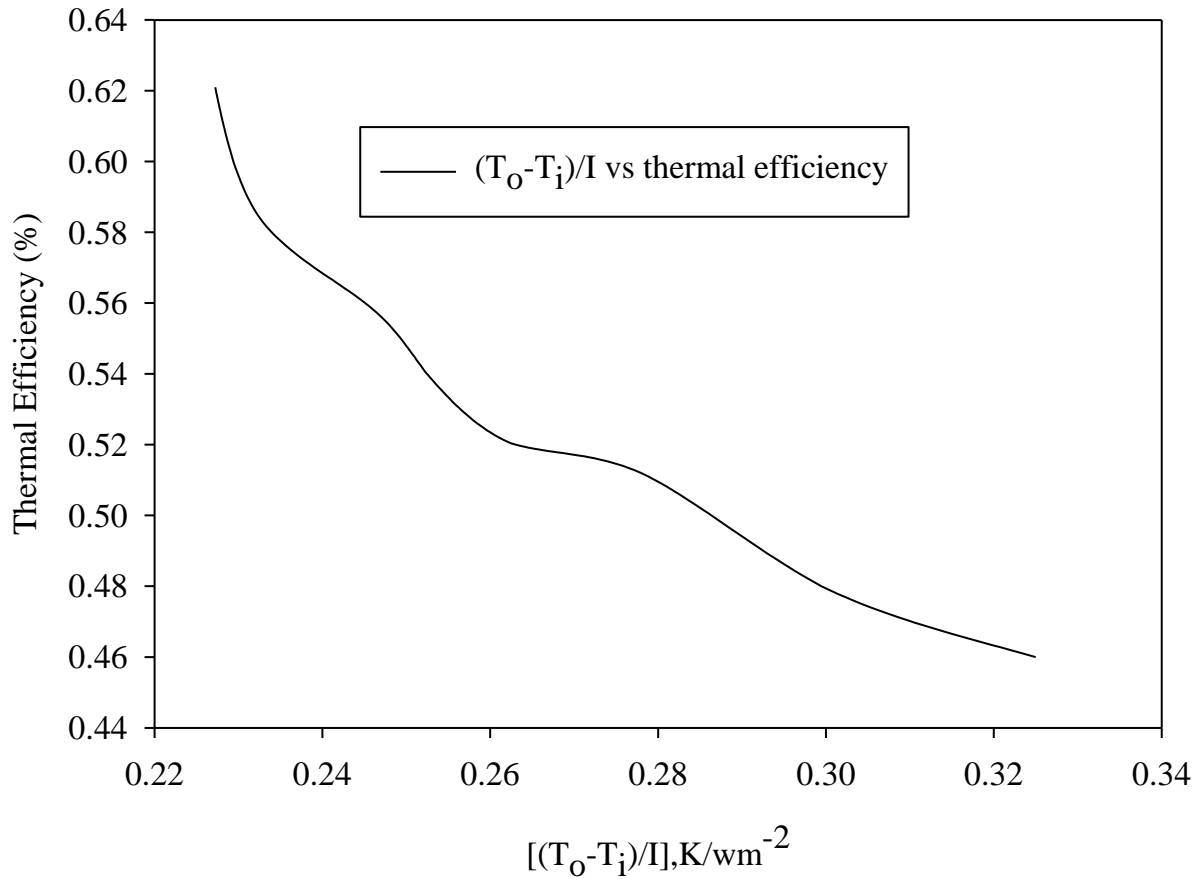
Figure 4.4 [T_o-T_i)/I] vs thermal efficiency graph

4.2 Development of governing equations and boundary conditions for baking pan

Discretization of the governing equations and the boundary conditions using one dimensional finite difference model as shown in Fig 4.5. can be expressed mathematically using explicitly finite difference. Generally, it will have three cases as internal node, first node and surface (nth) node.
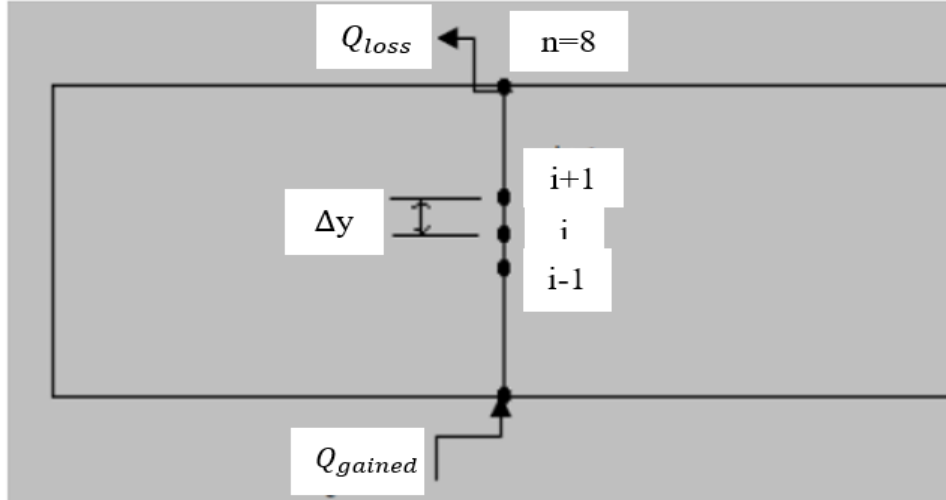
Figure 4.5 Discretize pan thickness using eight nodes[14]

Internal Node: the internal node has direct interactions with both of its neighboring nodes through conduction. The temperature of the node i at $t + 1$ time step is explicitly given as;

$$T_i^{t+1} = \tau \times \left(T_{i-1}^{\ t} - T_{i+1}^{\ t}\right) + (1 - 2\tau)T_i^{\ t} \qquad\qquad 4.1$$

Where $\tau = \dfrac{\alpha \Delta t}{\Delta y^2}$

$\alpha = \dfrac{k}{\rho c}$, heat diffusivity

t-represents the time step

Δt-Small time change of the total time for simulation

First Node: the first is in direct contact with the hot oil in the storage, the heat balance for the first node is given by[14]

$$h_{oc}\left(T_f - T_1^{\ t}\right) + k\frac{\left(T_2^{\ t} - T_1^{\ t}\right)}{\Delta y} = \rho\frac{\Delta y}{2}c_p\frac{\left(T_1^{\ t+1} - T_1^{\ t}\right)}{\Delta t} \qquad\qquad 4.2$$

Where h_{oc}- Hot oil to pan convection heat transfer coefficient

T_1-Temperature of the first node

T_f-The hot oil temperature

Δy-Differential thickness of pan

ρ-Density of oil

Δt-Differential time for computations

The temperature history of the first node can be expressed using explicit finite difference model is expressed by

$$T_1^{t+1} = \left(1 - 2\tau - 2\tau \frac{h_{oc}\Delta y}{k}\right) T_1^t + 2\tau\tau_1^t + 2\tau \frac{h_{oc}\Delta y}{k} T_f \qquad 4.3$$

The Top Surface (n^{th})Node: assuming that during heating up period of the baking pan the upper surface is exposed to air convection, and the effect of radiation heat transfer is negligible.
The heat balance at the node can be written explicitly as

$$h_a\left(T_\infty - T_n^t\right) + k \frac{\left(T_n^t - T_{n-1}^t\right)}{\Delta y} = \rho \frac{\Delta y}{2} c_p \frac{\left(T_n^{t+1} - T_n^t\right)}{\Delta t} \qquad 4.4$$

Where h_a-Air convection heat transfer coefficient

T_∞-Ambient air temperature

And the explicit finite difference temperature notation for the surface node (T_n) can be expressed as

$$T_n^{t+1} = \left(1 - 2\tau - 2\tau \frac{h_a\Delta y}{k}\right) T_n^t + 2\tau\tau_n^t + 2\tau \frac{h_a\Delta y}{k} T_\infty \qquad 4.5$$

The calculation of the convective heat transfer coefficients h_a and h_{oc} is based on the properties of air and hot oil at the corresponding film temperatures using Eq.3.5. The above three finite differences equations of nodes are used to simulate the temperature history of the baking surface for different changing parameters.

4.3 MATLAB Code for Pan Heat Transfer Using Explicit Finite Difference Approach

```
%-----------------------------------------------------

%Importing Material Property and Initial value

%-----------------------------------------------------

dy=0.001; % Differential Length, in meters

nn=8; % total Number of Nodes

k=0.45; % Thermal Conductivity of the Baking Pan, W/m K

cpc=880; %Specific Heat Capacity of Pan, J/Kg K

rho=1460; %Density of the Pan, Kg/m3

dt=1; %Time Step

alpha=k/(rho*cpc); %Thermal Diffusivity

tau=(alpha*dt)/(dx^2);

nts=3600; %Number of Time Step

Ta=25; %Ambient Temperature

Ta1 = 253; %Temperature of the Hot Oil

Ec=0.75; %Emissivity of the Pan

sigma=5.67*(10^(-8));%Stefan Boltzmann Constant

hbot=56.76; % Convection Coefficient Between the Hot oil and the Pan

htop=14.27;  % Convection Coefficient Between the air and the Pan

z2=((2*htop*dt)/(rho*dx*cpc));

z=(2*htop*dt/(rho*dx*cpc));

z1=(2*sigma*Ec*dt/(rho*cpc*dx));
```

```matlab
T=zeros(nn,nts+1); %initializing the solution matrix.

time(1)=0;

time=zeros(1,nts+1); %initializing the column vector containing successive time

% -------------------------------------------------------------

%Imposition of Initial Condition

%----------------------------------------------------

for i=1:nn;

T(i,1)=Ta; % The Initial Temperature of Baking Pan

end

%-------------------------------------------------------------------

% Evaluation of Temperature at Each Nodes Explicitly

%-------------------------------------------------------------------

for j=2:nts+1;

time(j)=dt*(j-1)/3600; %time given in hour

for i=2:nn-1;

T(i,j)=tau*(T(i-1,j-1)+ T(i+1,j-1))+((1-2*tau)*T(i,j-1));

end

T(1,j)=(1-(2*tau)-((2*tau*hbot*dx)/k))*T(1,j-1)+(2*tau*T(2,j-1))+((2*tau*hbot*dx)/k)*Ta1;

T(nn,j)=(1-(2*tau)-((2*tau*htop*dx)/k))*T(nn,j-1)+(2*tau*T(nn-1,j-
1))+((2*tau*htop*dx)/k)*Ta;

end

%-------------------------------------------------------------------

%Ploting the Results for Surface and Center Nodes
```

plot(time(1,:),'-r'); %plot for symmetric-center node of the rod

Table 4.2 Sample of MATLAB results

```
209.1884   209.1884   209.1884   209.1884   209.1884   209.1884   209.1884   209.1884   209.1884   209.1884   209.1884   209.1884
204.2812   204.2812   204.2812   204.2812   204.2812   204.2812   204.2812   204.2812   204.2812   204.2812   204.2812   204.2812
199.3741   199.3741   199.3741   199.3741   199.3741   199.3741   199.3741   199.3741   199.3741   199.3741   199.3741   199.3741
194.4669   194.4669   194.4669   194.4669   194.4669   194.4669   194.4669   194.4669   194.4669   194.4669   194.4669   194.4669
189.5598   189.5598   189.5598   189.5598   189.5598   189.5598   189.5598   189.5598   189.5598   189.5598   189.5598   189.5598
184.6526   184.6526   184.6526   184.6526   184.6526   184.6526   184.6526   184.6526   184.6526   184.6526   184.6526   184.6526
179.7455   179.7455   179.7455   179.7455   179.7455   179.7455   179.7455   179.7455   179.7455   179.7455   179.7455   179.7455


Columns 2989 through 3000


214.0955   214.0955   214.0955   214.0955   214.0955   214.0955   214.0955   214.0955   214.0955   214.0955   214.0955   214.0955
209.1884   209.1884   209.1884   209.1884   209.1884   209.1884   209.1884   209.1884   209.1884   209.1884   209.1884   209.1884
204.2812   204.2812   204.2812   204.2812   204.2812   204.2812   204.2812   204.2812   204.2812   204.2812   204.2812   204.2812
199.3741   199.3741   199.3741   199.3741   199.3741   199.3741   199.3741   199.3741   199.3741   199.3741   199.3741   199.3741
194.4669   194.4669   194.4669   194.4669   194.4669   194.4669   194.4669   194.4669   194.4669   194.4669   194.4669   194.4669
189.5598   189.5598   189.5598   189.5598   189.5598   189.5598   189.5598   189.5598   189.5598   189.5598   189.5598   189.5598
184.6526   184.6526   184.6526   184.6526   184.6526   184.6526   184.6526   184.6526   184.6526   184.6526   184.6526   184.6526
179.7455   179.7455   179.7455   179.7455   179.7455   179.7455   179.7455   179.7455   179.7455   179.7455   179.7455   179.7455


Columns 3001 through 3012


214.0955   214.0955   214.0955   214.0955   214.0955   214.0955   214.0955   214.0955   214.0955   214.0955   214.0955   214.0955
209.1884   209.1884   209.1884   209.1884   209.1884   209.1884   209.1884   209.1884   209.1884   209.1884   209.1884   209.1884
204.2812   204.2812   204.2812   204.2812   204.2812   204.2812   204.2812   204.2812   204.2812   204.2812   204.2812   204.2812
199.3741   199.3741   199.3741   199.3741   199.3741   199.3741   199.3741   199.3741   199.3741   199.3741   199.3741   199.3741
194.4669   194.4669   194.4669   194.4669   194.4669   194.4669   194.4669   194.4669   194.4669   194.4669   194.4669   194.4669
189.5598   189.5598   189.5598   189.5598   189.5598   189.5598   189.5598   189.5598   189.5598   189.5598   189.5598   189.5598
184.6526   184.6526   184.6526   184.6526   184.6526   184.6526   184.6526   184.6526   184.6526   184.6526   184.6526   184.6526
```

Figure 4.6 shows the temperature versus heating up time at difference thickness of the pan. The figure shows the temperature is increase with time, then it remains constant and decrease from bottom to surface. It shows that the pan thickness affects the heating time and the overall efficiency of the system. The maximum bottom temperature and surface temperature were 214.5 and 180(℃) which is attained after 10 to 15minutes.
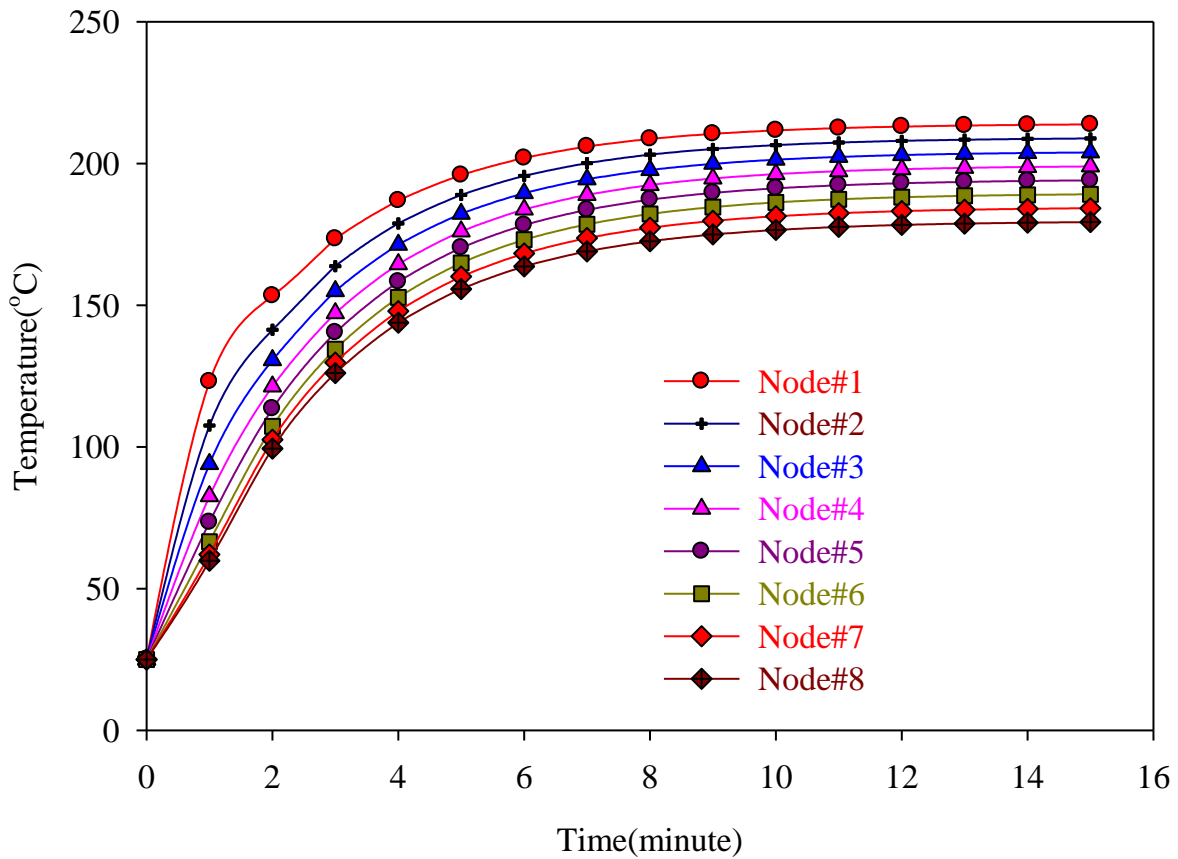
Figure 4.6 Heat up time versus temperature at different thickness of the pan

4.4   Heat up and retaining time of the pan surface

After the oil heated at the required temperature in the receiver and collected in the storage then the oil is allowed to flow for baking purpose. Temperature of the baking pan top surface starts to rise. In order to bake successfully, the top surface of the baking pan is expected to be at a temperature

of 180℃ to 220℃. Figure 4.7 shows the heating pan time and the baking pan surface temperature which the result comes in MATLAB manipulation. As it is seen in the figure, it takes approximately 10minutes to reach at the required temperature for baking.
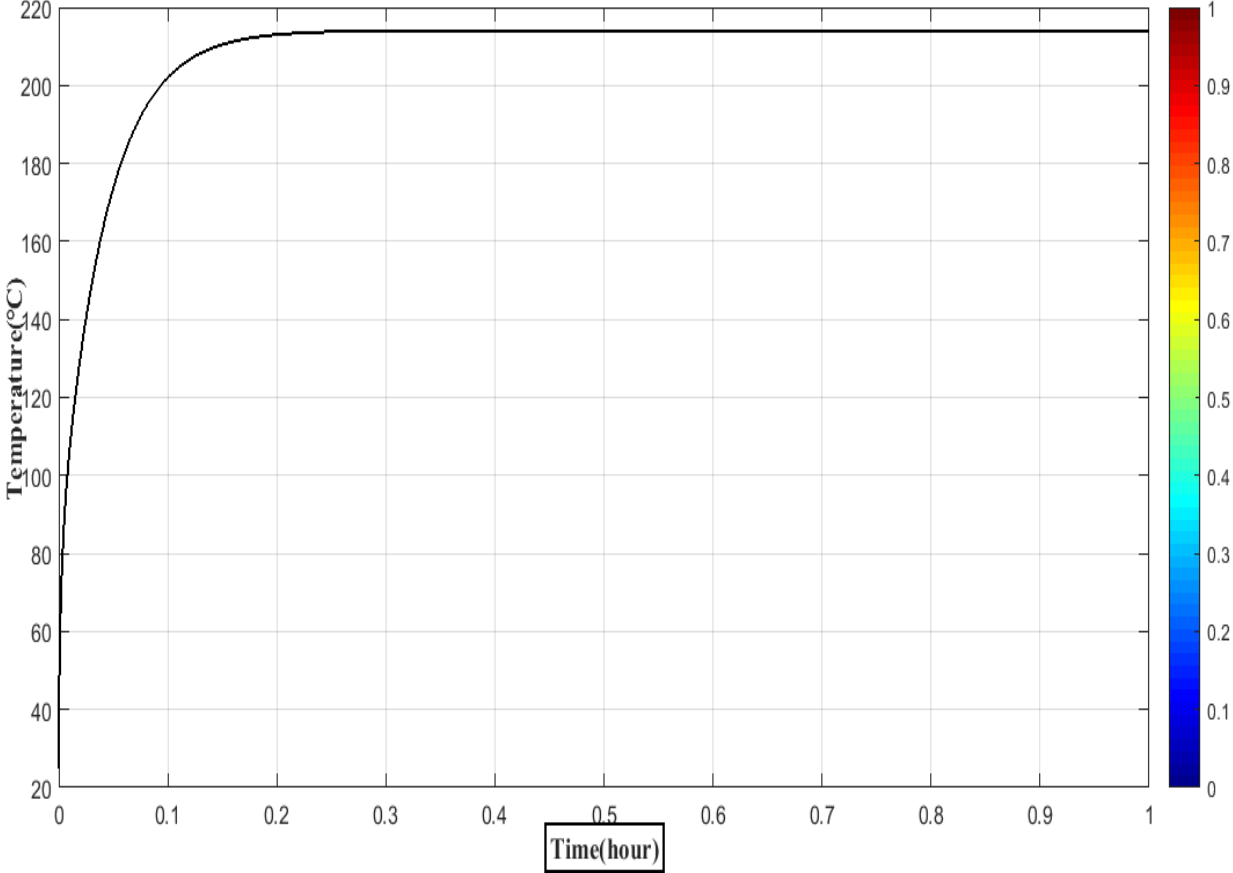
Figure 4.7 Heat up time and temperature distribution of baking pan surface

As show in the Figure 4.8 the temperature vs time graph indicates the time taken to recover the surface temperature of the pane after one lap which require less time than the heat up at the first time this is because the initial temperature of the first heating is 25℃ where as the surface temperature after one lap is 80℃ to 100℃.
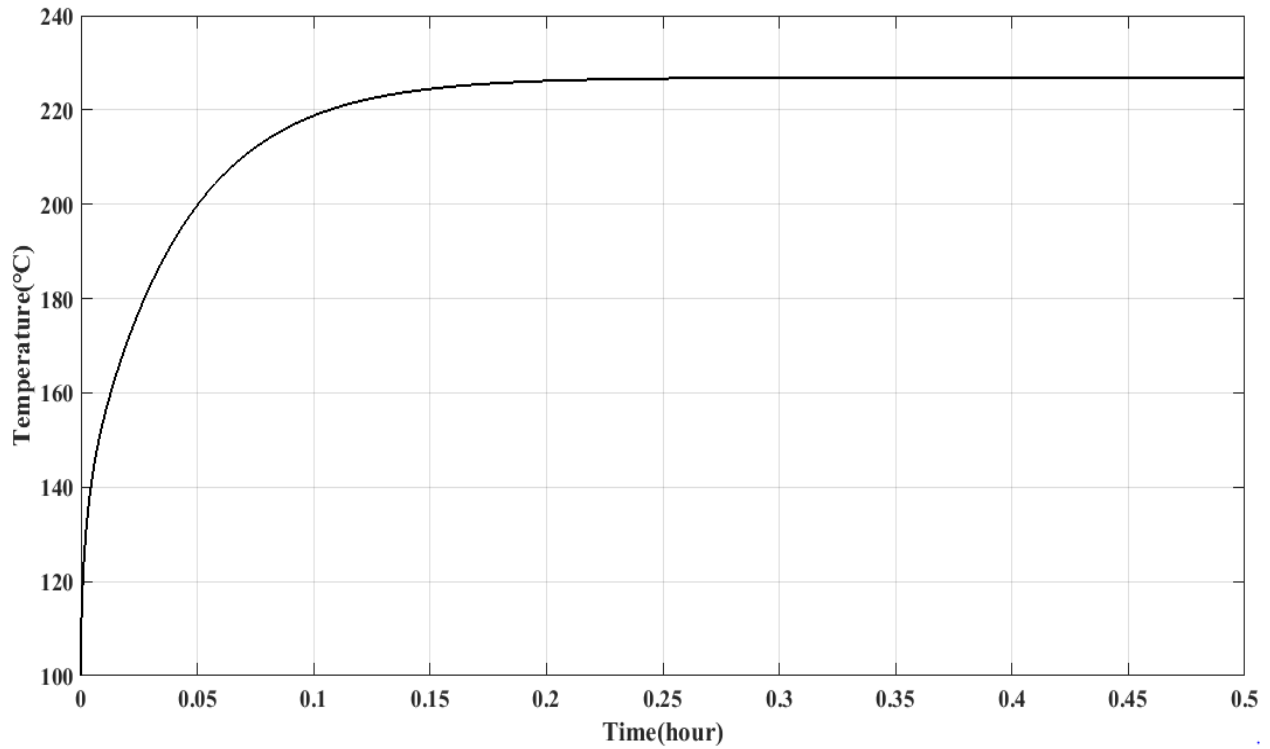
Figure 4.8 Retaining time after one baking lap

The baking pan surface transient temperature during heating and baking time as shown in Figure 4.9. the time require for first heating is 10-15minute to attain surface temperature around 200℃ then it will take 3-4minute for baking, then surface temperature will drop to 80-100℃. Where as the retaining time will be 3-5 minute and will reach up 200-220℃. And after one lap retaining time and baking time will be decrease.
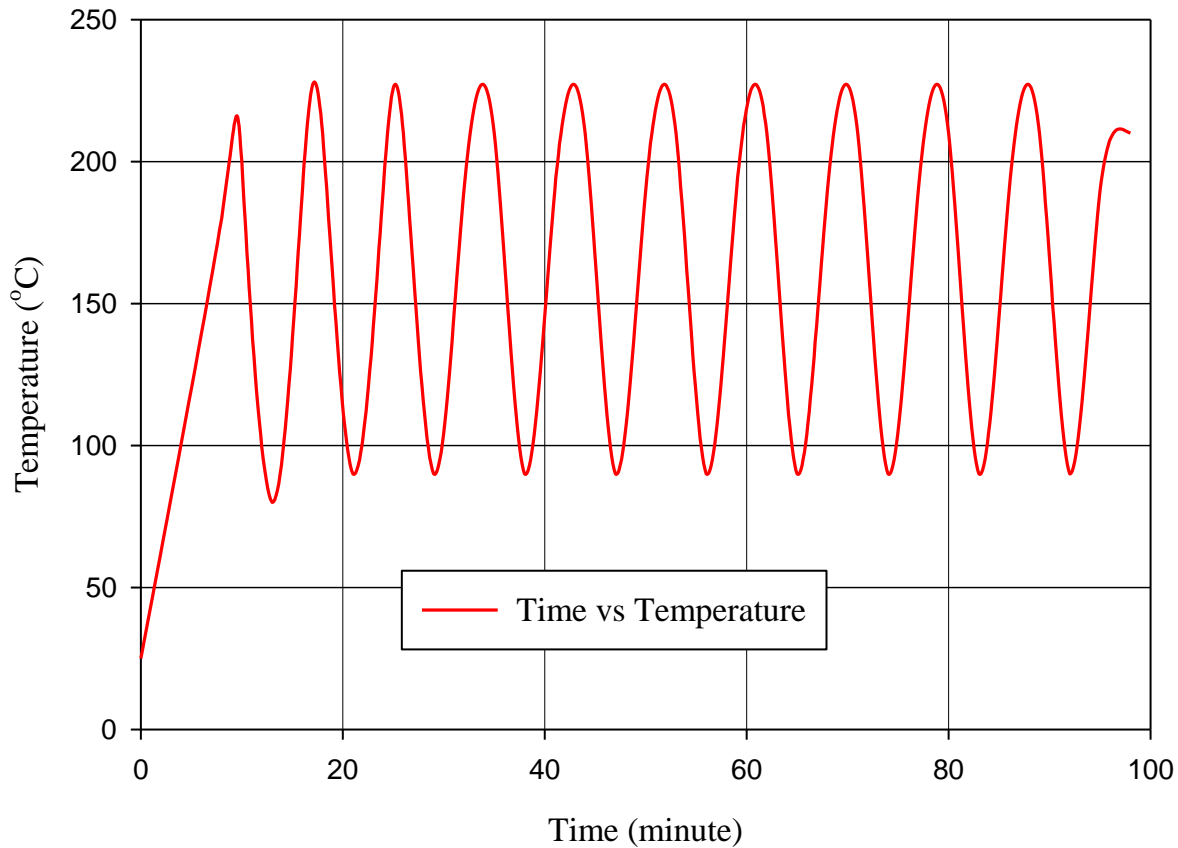
Figure 4.9 Heating, baking and retaining time versus temperature

4.5 Energy utilized for baking Injera

The energy utilized to bake injera is the energy required to raise the temperature of the dough (batter) to a particular temperature (sensible heat) and the amount of energy necessary to boil the water during the baking process (latent heat). The initial mass of batter and the mass of injera produced from the batter were measured to determine the energy required to cook injera. The mass of vapored water can be obtained by reducing the mass of injera produced from the initial mass of batter. It was assumed that, the heat capacity of the injera batter is the same as that of water during the sensible heating process. Therefore, the energy utilized for baking injera is given as:

$$E_{utilized} = m_{batter} \times C_P water \times (T_{boil} - T_{room}) + (m_{batter} - m_{Injera}) \times h_{vaporization}$$
4.6

73

Where; m_{batter} is the mass of the batter for one injera (0.4 kg), T_{boil} is the boiling temperature of water in Bahir Dare (94°C), T_{room} is the room temperature (25°C), C_P is the specific heat of water (4.187 kJ/kg.k), m_{Injera} is the mass of the injera produced (0.32kg), h_{fg} is the latent heat of vaporization of water (2260 kJ/kg). Based on these data the Energy utilized will be $\boldsymbol{459.615kJ}$. For baking time of 180 seconds, the power requirement during the baking of single injera becomes $2.553kW$.

4.6 Heat loss

Heat is transferred from the heating (receiver) to thermal storage to baking pan assembly by circulating heat transfer fluid through the pipe. Since the temperature of the fluid is much higher than ambient temperature, the fluid losses heat energy to ambient.

Heat is first lost from the heat transfer fluid through pipes wall by conduction and given as[68]:

$$P_{loss} = \frac{2\pi k_1 l}{ln\left(\frac{D_o}{D_i}\right)}\left[T_f - T_{pipe}\right] \qquad 4.7$$

Where: D_i and D_o are the inner (4.124mm) and outer diameters of the pipe (10.124mm) and k_1 is the thermal conductivity $(13W/m^2.K)$ of the pipe material.

Heat lost from the pipe through the insulation by conduction and radiation is given by

$$P_{loss} = \frac{2\pi k_2 l}{ln\left(\frac{D_o+2t}{D_i}\right)}\left[T_{pipe} - T_{amb}\right] + A_o\sigma\varepsilon_o\left(T_{pipe}{}^4 - T_{amb}{}^4\right) \qquad 4.8$$

Where k_2 is the thermal conductivity of the insulation material $(0.046\ W/m^2.K)$, t is the thickness of the insulation (2mm), A_o is the outer surface area of the pipe, D_o is the outside diameter of the pipe (10.124mm), l is length of the pipe (1.5m) , σ is the Stefan- Boltzmann constant, ε_o is the emittance of the outer surface of insulating material (0.04), $T_f, T_{pipe}\ and\ T_{amb}$ are average Oil temperature (250°C),Pipe outer wall temperature (40°C) and ambient temperature (25 °C) respectively. Based on these data the heat loss from pipe lines is 0.034kW.
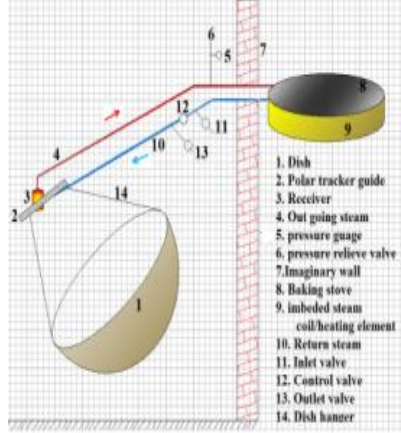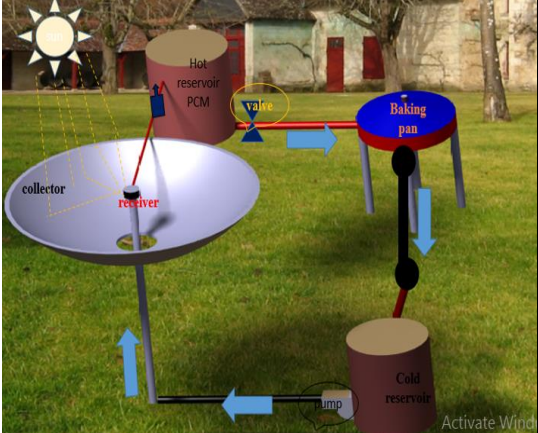
The heat loss in thermal storage insulated by Ash is ignored for this analysis. The Ash was found to be very effective insulator compared to fiber glass insulation. Hence the heat loss is calculated only for piping lines where fiber glass insulation was used.

4.7 Comparison of the present study from the previous works

Some researchers find different techniques of solar powered injera baking system design, modeling and experimental testing. For this work comparison is done with design and development of solar thermal injera baking: steam based direct baking (Asfafaw Haileselassie Tesfaye et al.2013). although the final target of the research is the same to this work but the mechanism and the output result of the two work is quantitatively having some difference as shown in the table 4.3.

Table 4.3 Comparison with previous work

	Literature	This research work
Comparator	Design and development of solar thermal injera baking: steam based direct baking (*Asfafaw Haileselassie Tesfaya et al.* 2013)	Design and experimental test of solar powered injera baking
Area of aperture (m^2)	2.8	2
Working fluid	Water	Thermal oil
Receiver type	Cylindrical type	Spiral coil copper pipe
Pan thickness, mm	10	5
Receiver temperature,T_r(℃)	350	306

	253	250
Fluid temperature, T_f (°C)	253	250
Heating up time	15	10-15
Baking mechanism	Direct baking	Indoor baking
Retaining time after one lap	15	3-5
Schematic drawing		

The other research work used for comparing was finite difference modelling of solar thermal powered injera baking oven (Desta Goytom,2016). This paper deals with simulation of transient heat transfer analysis of the solar powered injera baking system in which the heat transfer oil is heated using solar energy by parabolic trough and the oil circulates through the space below the baking -pan in the kitchen. The comparison is listed in Table 3.5

Table 4.4 Comparison with previous work on theoretical modeling

	Literature	This work
Comparator	Finite Difference Modelling of Solar Thermal Powered Injera Baking Oven (Desta Goytom,2016)	Design and experimental test of solar powered injera baking
Pan thickness, mm	5	5
Oil temperature (℃)	270	253
Heating up time (hour)	0.12	0.25
Pan bottom temperature (℃)	249.5	214.5
Pan surface temperature (℃)	200	179
Schematic diagram		

4.8 Economic Analysis

A reasonable cost of solar thermal injera baking system is an important factor to attract the user and increase its application for the replacement of other conventional baking options. In order to estimate the cost of solar thermal injera bakery, the cost of each material used for fabrication and the rental cost for professional and labor must be known.

4.8.1 Material cost

Table 4.5 List of material used to construct the setup corresponding with cost

Material	Use	Specification	Quantity	Unit price (ETB)	Total price (ETB)
Stainless steel sheet	Hot oil container inner wall and plate inside the pan	$1m \times 2m \times 2mm$	1	4000	4000
Stainless steel sheet	Cold oil container, thermal storage and small oil tank	$1m \times 2m \times 1mm$	1	2000	2000
Galvanized steel sheet	Storage outer wall construction	$1m \times 2m \times 1mm$	1	600	600
Adhesive (mastish)	To stick aluminum foil to parabolic dish		2	60	120
Aluminum foil	For covering parabolic dish	Roll	4	55	220

Aluminum sheet	Constructing receiver with copper spiral coil pipe	$1m \times 2m \times 1mm$	$^1/_8$	700	175
Corrugated steel sheet	For parabolic dish	$1m \times 2m \times 1mm$	4	200	800
Ange iron	For dish, storage and pan stand		2	300	600
Stainless steel electrode	For wilding of stainless to manufacturing of oil and salt storage	Packet	1	2000	2000
Pan	Baking injera	$\emptyset 0.5m \times 5mm$	1	200	200
Copper pipe	Spiral receiver fluid	$\emptyset 6mm$	4m	115	460
Steel pipe	Transporting fluid	$\emptyset\,^1/_4\,inch$	5m	250	1250
Control valve	Flow control	$\emptyset\,^1/_4 inch$	3	150	450
Elbow		$\emptyset\,^1/_4 inch$	3	200	600
pump	To pump oil from cold oil storage to receiver coil		1		2500
Potassium nitrate	Thermal storage	Kilogram	1.6	900	1440

Sodium nitrate	Thermal storage	Kilogram	2.4	580	1392
Glass wool	Insulated pipe	Pack	1	400	400
Painting	For paint storage and stand	Container	0.5 gallon	480	240
Thermal oil	Heat transfer fluid	Litters	12	200	2400
				Total	**21,847**

And the total manufacturing and assembling cost was around **4500 ETB**

Then the total baker cost can be calculated as:

$$Total\ intial\ cost = material\ cost + fibirication\ cost = \mathbf{26,347ETB}$$

Annual cost = Total initial cost + Maintenance cost + Operating cost − Salvage cost

Maintenance and operating cost =1000ETB

Salvage cost =10%intial cos =2634.7ETB

Annual cost=26,347ETB

4.8.2 Economic benefit of solar injera baker

Solar power injera baker will have economic and environmental benefit for the user. Although it has high initial cost relative to biomass and electric mitad but its operating and maintenance cost is relatively negligible. It also avoids healthy crisis that comes by using biomass baking system. Generally, this work will play great role for our country green policy.

Let's take a 5% interest rate which is the current interest rate of commercial bank of Ethiopia and the system can serve for a minimum of 10 years.

$$N = \frac{\sum M(n)}{(i+1)^n} \qquad\qquad 4.9$$

Equation used to calculate the present value of future money is

Where;

N - is the present value of future money.

M (n) - is the value of money after *n* years

n - is the number of years.

i -is the interest rate.

Using the above equation 4.9, the present value of the cost of the system N is

$$N = \frac{10 \times 1000 + 26{,}347}{(0.05 + 1)^{10}} = 22{,}313$$

The present value of the benefit of the system is calculated based current cost of wood is to bake as this system was 30ETB per day.

Annual cost of wood $= 30 \times 120 = 3600 ETB$

$$N = \frac{10 \times 3600 + 2634.7}{(0.05 + 1)^{10}} = 23{,}718 ETB$$

Net present value: The net present value (NPV) shows the economic gain that can be expected from the system in currency units of the base year. It is calculated by subtracting the economic costs of the system from the economic benefits.

$$NPV = present\ worth\ of\ benefit\text{-}\ present\ worth\ of\ cost$$

$$NPV = 23{,}718 - 22{,}313 = 1405 ETB$$

The benefit-cost ratio is equal to the present worth of benefit divided by the present worth of the cost of the system.

$$BCR = \frac{present\ worth\ of\ benefit}{present\ worth\ of\ t} = \frac{23{,}718}{22313} = 1.07$$

4.8.3 Payback period

The payback period (also termed the break-even point) is the period of time after which the benefits from system equal the total cost of system. It defines the point in time at which an intervention starts to produce net economic benefits.

$$Pay\ back\ period = \frac{The\ unit\ cost\ of\ the\ cooker}{cost\ saved}$$

$$Pay\ back\ period = \frac{22313}{3600} = 6.2$$

The payback period of solar powered injera baker is 6.2 year

CHAPTER FIVE

5 CONCLUSION AND RECOMMENDATION

5.1 Conclusion

Using renewable energy for baking and cooking process play a vital role in Scio-economic development of country like Ethiopia. High amount of energy with pan surface temperature of 180℃ to 220℃ is required for a single household to bake injera. Under theoretical and design consideration, this paper studies the amount of energy required for a single household is 18.38MJ of energy in one term baking. Parabolic dish type solar collector can extract more than 600℃, which is a best alternative to shift the country dependency on fossil fuel that causes environmental pollution. In this study design and experimental testing of solar thermal injera baking with thermal storage (PCM) has been carried out. During the experimental test ambient temperature (22-30℃), solar radiation (371-946$^W/_{m^2}$), receiver surface temperature (193-306℃) and fluid temperature (164-254℃) have been measured from 2:00-11:00 local time. Finally, the measured row data is analyzed using numerical method in MATLAB and sigma plot software.

The analysis result shows that, the thermal efficiency receiver (solar absorber) is 51.44%, the heat up time (time require to heat the pan initially) is 10-15 minute and the retaining time (heating time require after one lap) is 3-5 minute. The top and bottom surface temperature of the pan is 179.5 and 214.3℃ respectively.

Finally, although all the prototype is completely manufactured, leakage of fluid was difficult during experimental test, this is due to the reason that, all the experimental setup was manufactured by locally available materials and tools.

5.2   Recommendation

This work needs the following future improvements:

1. Designs need to incorporate thermostat and power regulator in order to achieve better safety and efficiency

2. Manufacturing with sophisticated technology have to be taken

3. Use automated tracking system

4. Use efficient reflected material like glass

REFERENCE

[1]   A. A. Hassen, S. B. Kebede, and N. M. Wihib, "Design and Manufacturing of Thermal Energy Based Injera Baking Glass Pan," *Energy Procedia*, vol. 93. pp. 154–159, 2016.

[2]   Abdulkadir A. Hassen1, Demiss A. Amibe1, Ole J.Nydal "Performance Investigation Of Solar Powered Injera Baking Oven For Indoor Cooking." .

[3]   M. H. Hailu, M. B. Kahsay, A. H. Tesfay, and O. I. Dawud, "Energy consumption performance analysis of electrical mitad at Mekelle City," *Momona Ethiop. J. Sci.*, 2017.

[4]   K. D. Adem and D. A. Ambie, "A review of injera baking technologies in Ethiopia: Challenges and gaps," *Energy for Sustainable Development*. 2017.

[5]   A. Y. Ali, "Design and Development of Semi-Automatic Injera Making Machine for Family Households in Ethiopia," 2018.

[6]   H. Weldekidan, V. Strezov, and G. Town, "Review of solar energy for biofuel extraction," *Renewable and Sustainable Energy Reviews*, vol. 88. pp. 184–192, 2018.

[7]   A. Haileselassie, M. Bayray, and O. Jørgen, "Design and development of solar thermal Injera baking : steam based direct baking," *Energy Procedia*, vol. 57, pp. 2946–2955, 2014.

[8]   A. H. Tesfay, O. J. Nydal, and M. B. Kahsay, "Energy storage integrated solar stove: A case of solar Injera baking in Ethiopia BT - 4th IEEE Global Humanitarian Technology Conference, GHTC 2014, October 10, 2014 - October 13, 2014." pp. 659–666, 2014.

[9]   *Asfafaw Haileselassie Tesfay Experimental Investigation of a Concentrating Solar Fryer Asfafaw Haileselassie Tesfay Experimental Investigation of a Concentrating Solar Fryer with Heat Storage*. 2015.

[10]   "ScienceNordic - Solar-powered bread baking in Ethiopia "http://sciencenordic.com/solar-powered-bread-baking-ethiopia- 2014-04-21.

[11] S. Indora and T. C. Kandpal, "Institutional cooking with solar energy : A review," *Renew. Sustain. Energy Rev.*, vol. 84, no. October 2017, pp. 131–154, 2018.

[12] A. Khelifa, K. Touafek, H. Ben Moussa, I. Tabet, H. B. C. El Hocine, and H. Haloui, "Analysis of a Hybrid Solar Collector Photovoltaic Thermal (PVT)," *Energy Procedia*, vol. 74. pp. 835–843, 2015.

[13] Y. Tavan, S. H. Hosseini, and G. Ahmadi, "Energy and Exergy Analysis of Intensified Condensate Stabilization Unit with Water Draw Pan," *Appl. Therm. Eng.*, 2019.

[14] D. Goytom, "Finite Difference Modelling of Solar Thermal Powered Injera Baking Oven," vol. 3, no. 12, 2016.

[15] I. L. Mohammed, "Design And Development Of A Parabolic Dish Solar Water Heater," vol. 2, no. 1, pp. 822–830, 2012.

[16] P. G. Scholar, "Design and Simulation of Parabolic Dish Collector for Hot Water Generation," no. 9, pp. 20–24, 2015.

[17] M. Gwani, G. A. Abubakar, M. Abbas, M. N. Allah, and J. Danyaro, "Design , Fabrication and Experimental Study of Solar Parabolic Dish Concentrator for Remote Area Application," vol. 4531.

[18] U. A. I. D. Technology, "High Temp Heat Transfer Fluids (250 C - 1000 C) for Use in Energy Capture Systems."

[19] J. Gasia, M. Martin, A. Solé, C. Barreneche, and L. Cabeza, "Phase Change Material Selection for Thermal Processes Working under Partial Load Operating Conditions in the Temperature Range between 120 and 200 °C," *Applied Sciences*, vol. 7, no. 7. p. 722, 2017.

[20] F. Kenfack and M. Bauer, "Innovative Phase Change Material (PCM) for heat storage for industrial applications," *Energy Procedia*, vol. 46. pp. 310–316, 2014.

[21] Ramesh K. Shah and Dušan P. Sekulic, "Fundamentals of Heat Exchanger Design" 2003 New York.

[22] P. Technique, N. Technical, and P. Technique, "Design , Simulation , And Optimization Of A Solar Dish Collector With Spiral-Coil Thermal Absorber," 2016.

[23] J. A. Alarcón, J. E. Hortúa, and A. L. G, "Design and construction of a solar collector parabolic dish for rural zones in Colombia Diseño y construcción de un colector solar parabólico tipo disco para zonas rurales," vol. 7, no. 14, pp. 14–22, 2013.

[24] J. D. Osorio and A. Rivera-Alvarez, "Performance analysis of Parabolic Trough Collectors with Double Glass Envelope," *Renew. Energy*, 2019.

[25] Q. C. Zhang and D. R. Mills, "High solar performance selective surface using bi-sublayer cermet film structures," *Sol. Energy Mater. Sol. Cells*, 1992.

[26] R. Kumar, A. Kumar, and V. Goel, "Performance improvement and development of correlation for friction factor and heat transfer using computational fluid dynamics for ribbed triangular duct solar air heater," *Renew. Energy*, 2019.

[27] W. Kong *et al.*, "Test method for evaluating and predicting thermal performance of thermosyphon solar domestic hot water system," *Appl. Therm. Eng.*, 2019.

[28] " Energy Policy Of The Transitional Government Of Ethiopia 1. Preamble."

[29] A. Nahar, M. Hasanuzzaman, N. A. Rahim, and S. Parvin, "Numerical investigation on the effect of different parameters in enhancing heat transfer performance of photovoltaic thermal systems," *Renew. Energy*, 2019.

[30] S. Y. Heng, Y. Asako, T. Suwa, and K. Nagasaka, "Transient thermal prediction methodology for parabolic trough solar collector tube using artificial neural network," *Renew. Energy*, 2019.

[31] Getahun Moges "Electric Injera Mitad Energy Efficiency Standards & Labeling, challenges and prospects." EEA,2017

[32] H. Z. Al Garni, A. Awasthi, and D. Wright, "Optimal orientation angles for maximizing energy yield for solar PV in Saudi Arabia Optimal orientation angles for maximizing 1 energy yield for solar PV in Saudi Arabia 2 3," *Renew. Energy*, 2018.

[33] M. S. Dehaj and M. Z. Mohiabadi, "Experimental investigation of heat pipe solar collector using MgO nanofluids," *Sol. Energy Mater. Sol. Cells*, 2019.

[34] O. Z. Sharaf, A. N. Al-Khateeb, D. C. Kyritsis, and E. Abu-Nada, "Energy and exergy analysis and optimization of low-flux direct absorption solar collectors (DASCs): Balancing power- and temperature-gain," *Renew. Energy*, 2019.

[35] H. M. K. U. Haq and E. Hiltunen, "An inquiry of ground heat storage: Analysis of experimental measurements and optimization of system's performance," *Appl. Therm. Eng.*, 2019.

[36] A. Abdessemed, C. Bougriou, D. Guerraiche, and R. Abachi, "Effects of tray shape of a multi-stage solar still coupled to a parabolic concentrating solar collector in Algeria," *Renew. Energy*, 2019.

[37] A. Bianchini, A. Guzzini, M. Pellegrini, and C. Saccani, "Performance assessment of a solar parabolic dish for domestic use based on experimental measurements," *Renew. Energy*, 2019.

[38] P. A. González-Gómez, J. Gómez-Hernández, D. Ferruzza, F. Haglind, and D. Santana, "Dynamic performance and stress analysis of the steam generator of parabolic trough solar power plants," *Appl. Therm. Eng.*, 2019.

[39] M. Malekan, A. Khosravi, and X. Zhao, "The influence of magnetic field on heat transfer

of magnetic nanofluid in a double pipe heat exchanger proposed in a small-scale CAES system," *Appl. Therm. Eng.*, 2019.

[40] S. Marrakchi, Z. Leemrani, H. Asselman, A. Aoukili, and A. Asselman, "Temperature distribution analysis of parabolic trough solar collector using CFD," in *Procedia Manufacturing*, 2018.

[41] O. V. Shepovalova, V. A. Chuzhmarov, A. V. Pismenov, and D. A. Durnev, "Special High-Temperature Solar Collector in Off-Grid Energy Systems for Stand-Alone Buildings and Settlements," in *Energy Procedia*, 2015.

[42] A. H. Tesfay, M. B. Kahsay, and O. J. Nydal, "Solar powered heat storage for Injera baking in Ethiopia," in *Energy Procedia*, 2014.

[43] N. L. Panwar, S. C. Kaushik, and S. Kothari, "State of the art of solar cooking: An overview," *Renewable and Sustainable Energy Reviews*. 2012.

[44] L. Nkhonjera, T. Bello-Ochende, G. John, and C. K. King'ondu, "A review of thermal energy storage designs, heat storage materials and cooking performance of solar cookers with heat storage," *Renewable and Sustainable Energy Reviews*. 2017.

[45] A. Shahsavar and S. Khanmohammadi, "Feasibility of a hybrid BIPV/T and thermal wheel system for exhaust air heat recovery: Energy and exergy assessment and multi-objective optimization," *Appl. Therm. Eng.*, 2019.

[46] J. Qu, R. Zhang, Z. Wang, and Q. Wang, "Photo-thermal conversion properties of hybrid CuO-MWCNT/H2O nanofluids for direct solar thermal energy harvest," *Appl. Therm. Eng.*, 2019.

[47] M. Ahmadi, S. Vahaji, M. Arbab Iqbal, A. Date, and A. Akbarzadeh, "Experimental study of converging-diverging nozzle to generate power by Trilateral Flash Cycle (TFC)," *Appl.*

Therm. Eng., 2019.

[48]   Y. Liu, Y. Chen, Y. Zhou, D. Wang, Y. Wang, and D. Wang, "Experimental research on the thermal performance of PEX helical coil pipes for heating the biogas digester," *Appl. Therm. Eng.*, 2019.

[49]   E. Bellos, I. Daniil, and C. Tzivanidis, "Multiple cylindrical inserts for parabolic trough solar collector," *Appl. Therm. Eng.*, 2018.

[50]   F. Zhou, J. Ji, W. Yuan, M. Modjinou, X. Zhao, and shengjuan Huang, "Experimental study and performance prediction of the PCM-antifreeze solar thermal system under cold weather conditions," *Appl. Therm. Eng.*, 2019.

[51]   S. Şevik and M. Abuşka, "Thermal performance of flexible air duct using a new absorber construction in a solar air collector," 2018.

[52]   H. Jia, X. Cheng, J. Zhu, Z. Li, and J. Guo, "Mathematical and experimental analysis on solar thermal energy harvesting performance of the textile-based solar thermal energy collector," *Renew. Energy*, 2018.

[53]   M. Imtiaz Hussain, C. Ménézo, and J. T. Kim, "Advances in solar thermal harvesting technology based on surface solar absorption collectors: A review," *Sol. Energy Mater. Sol. Cells*, 2018.

[54]   D. V. Bellas and E. Lidorikis, "Design of high-temperature solar-selective coatings for application in solar collectors," *Sol. Energy Mater. Sol. Cells*, 2017.

[55]   U. R. Prasanna and L. Umanand, "Optimization and design of energy transport system for solar cooking application," *Appl. Energy*, 2011.

[56]   B. Agza, R. Bekele, and L. Shiferaw, "Quinoa (Chenopodium quinoa, Wild.): As a potential ingredient of injera in Ethiopia," *J. Cereal Sci.*, 2018.

[57]　G. Kumaresan, R. Santosh, G. Raju, and R. Velraj, "Experimental and numerical investigation of solar flat plate cooking unit for domestic applications," *Energy*, 2018.

[58]　A. Aichouba, M. Merzouk, L. Valenzuela, E. Zarza, and N. Kasbadji-Merzouk, "Influence of the displacement of solar receiver tubes on the performance of a parabolic-trough collector," *Energy*, 2018.

[59]　L. Xu *et al.*, "Analysis of the influence of heat loss factors on the overall performance of utility-scale parabolic trough solar collectors," *Energy*, 2018.

[60]　Y. Assefa, S. Emire, M. Villanueva, W. Abebe, and F. Ronda, "Influence of milling type on tef injera quality," *Food Chem.*, 2018.

[61]　F. E. B. Bioucas, S. I. C. Vieira, M. J. V. Lourenço, F. J. V. Santos, and C. A. Nieto de Castro, "Performance of heat transfer fluids with nanographene in a pilot solar collector," *Solar Energy*, 2018.

[62]　B. Schiebler, H. Dieckmann, F. Giovannetti, and S. Jack, "Experimental and theoretical investigations on temperature limitation in solar thermal collectors with heat pipes: Effect of superheating on the maximum temperature," *Sol. Energy*, 2018.

[63]　A. H. Tesfay, M. B. Kahsay, and O. J. Nydal, "Design and development of solar thermal Injera baking: Steam based direct baking," in *Energy Procedia*, 2014.

[64]　Stanley.A. and Matthews, D , "Alternative energy sources (solar energy)." Solar Enewv. 1995

[65]　A. Gallagher, "A solar fryer," *Sol. Energy*, 2011.

[66]　G. Zubi, F. Spertino, M. Carvalho, R. S. Adhikari, and T. Khatib, "Development and assessment of a solar home system to cover cooking and lighting needs in developing regions as a better alternative for existing practices," *Sol. Energy*, 2017.

[67]   I. Edmonds, "Low cost realisation of a high temperature solar cooker," *Renew. Energy*, vol. 121, pp. 94–101, 2018.

APPENDIX A

Table A 1 Result of experimental test

Time	Ambient temperature (°C)			Solar radiation($^{W}/_{m^2}$)			Receiver surface temperature (°C)			Receiver outlet Fluid temperature (°C)		
	Day#1	Day#2	Day#3	Day#1	Day#2	Day#3	Day#1	Day#2	Day#3	Day#1	Day#2	Day#3
8:00	22.3	21.3	22.20	359	371	368	187.23	193.32	196.2	157.3	162.25	163.2
9:00	23.9	23.8	24.3	518	523	530	205.63	209.45	211.36	174.69	185.15	182.63
10:00	25.6	25.1	26.3	763	768	759	267.3	277.4	283.12	213.74	217.2	221.36
11:00	26.67	25.7	27.4	789	805	793	278.9	289.4	291.35	229.91	238.27	240.05
12:00	27.4	27.2	27.6	886	893	888	291.37	293.89	293.67	237.5	242.7	241.89
1:00	28.2	28.3	28.4	918	922	916	301.2	305.6	306.6	243.57	247.78	248.87
2:00	28.93	28.8	29.1	939	946	935	307.25	310.5	311.3	245.68	250.09	253.91
3:00	28.3	27.4	28.2	880	896	875	291.2	283.54	304.2	219.45	223.58	246.35
4:00	25.6	25.5	25.4	715	712	719	257.58	262.87	261.3	207.85	210.94	209.13
5:00	23.7	23.6	23.8	370	368	375	249.35	260.35	260.02	203.38	207.27	207.02
AVG	26.06	25.67	26.27	713.7	720.4	715.8	257.70	268.63	271.21	213.307	218.523	221.14

Table A 2 First heating time of the pan at different thickness of the pan

Time (minute)	Nodal temperature of pan at different thickness (℃)							
	node#1	node#2	node#3	node#4	node#5	node#6	node#7	node#8
0	25	25	25	25	25	25	25	25
1	123.0248	107.5173	93.9856	82.5857	73.4261	66.5695	62.0361	59.8073
2	153.2909	141.2942	130.5928	121.2969	113.4904	107.2284	102.5366	99.4109
3	173.4262	163.7772	154.9943	147.1515	140.3048	134.4911	129.7279	126.0122
4	186.8934	178.8146	171.3151	164.4444	158.24	152.7265	147.9156	143.8054
5	195.9011	188.8725	182.2315	176.011	170.2361	164.9234	160.0806	155.7065
6	201.926	195.5999	189.533	183.7474	178.2599	173.0815	168.2174	163.6668
7	205.9558	200.0996	194.4167	188.922	183.6267	178.5381	173.6597	168.991
8	208.6512	203.1092	197.6832	192.3831	187.2163	182.1878	177.2999	172.5523
9	210.454	205.1223	199.8681	194.6981	189.6173	184.6289	179.7347	174.9342
10	211.6599	206.4687	201.3294	196.2465	191.2232	186.2617	181.3632	176.5274
11	212.4664	207.3693	202.3069	197.2821	192.2973	187.3538	182.4525	177.593
12	213.0059	207.9717	202.9607	197.9749	193.0157	188.0843	183.181	178.3058
13	213.3667	208.3746	203.398	198.4382	193.4963	188.5729	183.6683	178.7825
14	213.608	208.6441	203.6904	198.7481	193.8177	188.8997	183.9943	179.1014
15	213.7695	208.8243	203.8861	198.9554	194.0327	189.1183	184.2123	179.3147

APPENDIX B

Table B 1 Solar Radiation Data Collected from National Metrology

በበሔራዊ የሚቲዎሮሎጂ ኤጀንሲ
የምዕራብ አማራ ሚቲዎሮሎጂ
አገልግሎት ማዕከል

National Meteorology Agency
Western Amhara Meteorological
Services Center

ቁጥር.....................
RefNo

ቀን......................
Date

Solar Radiation average data (4:00 -11:00) In (w/m2)													
Year	Date	Jan	Feb	Mar	Apr	May	Jun	Jul	Aug	Sep	Oct	Nov	Dec
2014	1	720.1	812.4	906.5	889.9	721.7	900.5	819.5	247.6	562.8	883.9	823.6	771.6
	2	752.6	811.2	886.4	938.9	835.2	547.8	810.2	472.7	878.6	679.5	824.6	764.0
	3	743.3	681.5	921.6	871.0	910.1	806.6	884.3	870.1	865.7	798.8	788.3	764.4
	4	771.0	815.9	620.9	244.4	881.2	829.3	302.2	323.0	740.3	529.6	816.9	775.1
	5	735.4	816.7	784.7	608.7	511.6	229.6	833.1	215.7	922.6	872.8	814.3	777.6
	6	747.0	831.5	892.3	915.6	840.4	517.6	853.6	445.0	196.1	830.6	839.7	762.9
	7	717.2	817.1	899.4	214.1	869.0	624.1	837.4	311.2	946.4	903.1	796.9	744.7
	8	711.5	829.0	890.4	946.2	510.8	815.4	746.4	602.5	104.6	355.3	793.8	734.1
	9	694.3	814.2	908.7	708.0	322.0	843.1	715.8	930.2	844.8	858.0	802.2	723.4
	10	723.6	815.4	913.4	296.8	885.1	837.5	389.7	1075.0	275.6	909.3	806.9	750.2
	11	726.9	798.4	793.8	384.4	645.1	800.6	722.4	893.8	884.6	386.2	799.1	770.6
	12	735.0	862.3	898.9	877.9	862.1	805.6	912.0	156.7	912.2	863.7	798.7	767.9
	13	736.1	858.3	914.9	886.5	869.4	820.6	818.0	587.4	520.5	885.8	775.6	769.9
	14	737.5	853.8	906.5	952.0	875.2	831.5	822.4	883.9	385.7	778.9	808.5	754.5
	15	738.1	843.1	888.6	914.6	692.0	818.4	685.0	649.9	219.1	718.1	768.3	725.0

95

	Date	Jan	Feb	Mar	Apr	May	Jun	Jul	Aug	Sep	Oct	Nov	Dec
	16	739.9	804.9	904.9	919.8	840.7	832.8	845.3	851.0	562.3	852.9	781.8	727.9
	17	748.6	755.2	446.2	892.3	847.0	845.6	771.0	863.2	938.4	860.4	769.1	707.2
	18	770.8	584.7	913.4	863.8	404.9	825.7	798.0	901.1	939.3	866.3	778.0	736.0
	19	741.9	877.1	910.3	892.2	852.3	883.6	818.9	514.5	155.5	602.5	776.9	816.4
	20	765.1	884.6	908.1	906.9	854.7	812.9	828.1	839.2	879.3	838.3	733.3	760.4
	21	773.4	864.8	916.2	938.9	844.2	171.1	554.0	923.2	858.0	842.1	719.9	762.5
	22	785.6	863.3	885.7	871.7	304.1	581.5	942.9	776.5	763.2	854.4	778.9	765.2
	23	806.1	901.5	893.1	506.5	NA	820.8	474.1	709.9	888.7	847.6	776.3	743.8
	24	737.1	890.9	890.6	891.7	NA	598.3	199.5	855.0	869.0	838.4	776.5	754.0
	25	829.1	873.8	895.2	850.6	NA	834.8	488.8	833.1	872.6	844.7	765.8	710.6
	26	790.4	887.6	912.0	873.2	NA	820.3	768.8	253.1	859.1	841.7	763.2	699.4
	27	682.0	886.2	897.7	534.8	NA	295.8	777.9	427.4	885.5	829.8	736.9	735.6
	28	781.8	855.1	893.4	916.3	NA	874.9	644.1	874.0	879.7	848.4	771.7	756.6
	29	707.4		910.4	785.8	NA	800.8	31.3	574.9	864.0	835.6	748.7	770.6
	30	794.7		920.0	884.2	855.5	821.2	742.4	875.7	863.5	829.9	753.9	789.7
	31	829.3		906.0		274.7		618.6	773.6		837.0		787.6
Year	Date	Jan	Feb	Mar	Apr	May	Jun	Jul	Aug	Sep	Oct	Nov	Dec
2015	1	780.5	887.6	884.1	898.8	842.9	939.9	821.0	829.4	632.4	874.3	506.5	769.1
	2	795.4	892.7	876.0	892.2	845.3	835.0	759.8	819.6	867.3	901.5	828.8	755.4
	3	790.3	882.9	878.1	895.6	946.9	871.3	817.4	678.0	429.6	863.9	758.7	762.0
	4	792.2	884.7	904.7	860.3	486.8	834.7	816.4	842.8	138.5	873.5	704.1	768.7
	5	767.7	863.7	877.0	877.6	878.6	506.1	768.6	460.5	555.9	854.9	797.7	753.9
	6	753.1	871.1	856.5	772.0	889.2	134.5	801.8	574.1	578.7	849.6	828.4	744.3
	7	754.1	851.0	867.1	860.7	827.8	807.2	810.0	776.5	852.6	549.5	850.9	558.8
	8	761.5	848.2	892.6	877.5	876.2	614.5	815.9	773.8	779.4	843.7	830.8	764.5
	9	754.7	877.5	896.3	876.7	866.2	496.8	786.3	879.8	53.7	850.5	810.7	514.4
	10	758.4	853.9	899.2	883.8	112.1	763.6	794.0	747.0	883.8	838.6	802.7	496.4
	11	718.9	863.3	889.4	880.3	927.4	789.7	803.8	845.3	877.6	281.5	800.5	754.3
	12	753.0	853.0	875.5	858.2	683.9	745.1	806.0	666.7	878.1	611.6	802.2	757.2
	13	720.7	870.9	874.6	853.2	884.1	766.9	199.4	840.5	619.3	845.4	699.6	772.3

	14	758.7	857.0	884.9	884.7	873.2	801.3	740.4	827.0	910.7	361.6	808.5	767.3
	15	775.1	847.7	901.3	851.0	864.7	792.8	833.8	830.3	786.0	818.7	824.4	770.1
	16	778.5	843.1	899.5	863.2	850.8	802.2	832.6	673.8	899.2	849.4	795.4	742.9
	17	795.7	840.6	351.0	852.2	709.5	342.6	789.9	839.1	878.2	833.3	810.9	731.3
	18	782.7	858.8	871.2	914.7	867.8	704.1	737.5	802.0	769.8	814.8	796.9	726.2
	19	761.6	868.7	908.7	889.1	961.7	809.0	853.1	763.6	216.2	553.3	789.9	784.5
	20	755.7	862.7	929.1	881.2	775.6	792.9	828.2	663.2	832.9	844.2	796.9	765.4
	21	755.2	863.5	863.7	907.9	889.4	778.1	834.5	756.2	861.5	725.0	789.3	776.1
	22	765.0	871.6	910.8	885.9	830.0	352.7	831.1	258.6	619.3	831.7	804.5	754.5
	23	790.6	866.3	900.6	892.0	833.3	762.8	855.3	997.6	849.7	839.2	791.7	765.1
	24	796.4	880.4	935.6	883.1	835.4	823.2	899.7	729.4	468.8	821.3	799.5	756.4
	25	789.3	891.5	905.8	926.8	831.0	833.0	825.9	449.4	69.0	674.5	780.5	757.6
	26	857.2	877.5	907.1	850.2	831.1	822.5	812.9	523.1	537.7	819.6	762.6	741.9
	27	851.5	872.9	913.8	841.2	872.2	687.4	833.6	788.7	827.4	832.3	837.7	731.1
	28	852.5	885.5	910.7	849.3	752.7	898.4	822.9	950.2	879.9	807.0	751.7	771.2
	29	882.4		906.5	907.7	855.2	876.6	767.4	786.5	858.4	614.2	785.8	762.8
	30	891.1		914.1	868.1	838.4	865.7	867.1	864.1	867.4	827.1	778.1	475.3
	31	890.8		895.0		840.8		849.8	613.3		804.5		751.3
2016	1	735.5	793.2	756.9	788.5	854.6	811.8	775.8	960.0	848.2	846.6	831.3	675.0
	2	723.3	791.1	878.5	885.1	709.4	815.1	781.6	491.6	925.0	855.4	822.3	727.6
	3	758.5	820.8	811.9	869.7	839.5	803.2	777.8	1014.0	624.8	710.1	806.4	760.3
	4	757.9	807.3	855.3	847.3	878.0	814.9	799.4	903.9	875.8	846.5	836.2	766.5
	5	725.1	811.3	854.9	879.4	185.6	865.8	284.3	185.8	853.9	824.8	800.9	773.2
	6	413.0	823.8	830.9	870.1	664.2	144.7	302.2	292.1	762.5	849.9	789.6	769.0
	7	758.2	818.0	858.4	864.2	599.7	118.8	362.6	534.8	834.4	710.9	786.7	742.1
	8	750.0	814.3	869.2	869.7	868.1	790.5	60.2	30.2	681.6	831.9	634.2	750.7
	9	773.3	815.4	875.0	865.3	856.2	149.5	460.4	541.6	704.6	821.5	477.0	736.6
	10	779.9	800.4	850.7	853.9	565.8	855.2	682.5	524.7	680.3	838.4	589.0	736.1
	11	773.2	808.7	889.0	855.2	429.9	302.0	101.2	789.4	691.7	831.5	543.6	720.5
	12	761.9	808.0	874.7	590.3	729.0	817.7	824.3	828.0	395.2	420.5	805.0	551.2

	13	735.9	810.5	795.9	417.1	854.5	733.3	323.5	823.6	836.2	829.1	816.6	740.6
	14	766.9	822.6	881.4	816.4	845.1	805.3	881.5	838.2	836.1	818.2	801.4	736.6
	15	737.6	831.7	864.2	831.5	861.1	148.4	302.8	839.5	841.2	823.7	782.8	746.8
	16	747.6	824.0	871.5	834.9	849.7	747.8	804.6	833.9	894.6	829.1	766.5	728.8
	17	752.4	808.9	857.9	366.4	438.2	821.6	119.4	562.8	551.3	833.1	765.9	746.0
	18	748.7	800.1	629.0	836.3	836.8	577.5	769.2	828.0	842.9	798.4	762.7	743.2
	19	739.7	825.7	898.4	862.1	823.6	333.9	872.5	330.6	532.5	818.8	756.0	771.3
	20	691.6	839.6	958.7	683.0	826.5	688.2	691.2	216.8	726.0	808.1	747.5	742.0
	21	759.4	846.6	617.3	857.3	824.4	779.8	302.8	878.2	517.6	836.1	773.4	746.3
	22	750.2	802.2	860.3	517.2	833.8	744.2	213.3	842.1	841.8	804.8	746.7	735.1
	23	744.4	793.6	915.2	867.4	839.5	585.2	781.5	846.9	851.5	812.3	759.9	765.1
	24	774.5	801.3	883.7	874.4	822.5	765.0	154.3	838.0	839.1	590.2	728.8	748.7
	25	785.9	803.0	892.0	871.2	822.4	782.5	818.2	659.5	748.0	621.5	735.7	769.8
	26	778.3	838.1	897.4	860.9	831.2	765.6	751.7	386.5	889.4	804.4	702.4	817.5
	27	795.7	846.5	894.5	678.5	824.4	781.6	106.2	686.0	545.2	790.0	702.7	791.6
	28	770.5	877.5	887.7	815.1	839.9	774.9	395.2	844.9	840.4	786.4	724.2	813.8
	29	793.7	882.2	858.5	411.9	826.0	627.7	805.8	859.8	776.5	827.0	749.9	778.7
	30	793.9		871.7	437.4	224.3	779.4	573.9	716.9	850.8	809.3	754.6	779.2
	31	740.5		872.8		814.6		843.7	159.9		819.7		770.7
Year	Date	Jan	Feb	Mar	Apr	May	Jun	Jul	Aug	Sep	Oct	Nov	Dec
2017	1	782.7	807.0	857.0	953.8	687.8	795.0	729.4	719.4	655.2	743.3	790.1	756.6
	2	790.0	806.9	855.6	744.5	771.0	785.8	392.9	823.9	676.5	704.2	795.5	750.4
	3	792.6	811.6	851.0	880.9	689.5	763.1	801.4	835.2	863.6	861.3	771.5	487.5
	4	798.3	801.6	832.4	877.4	661.9	775.1	278.0	463.9	112.4	501.9	681.3	743.3
	5	817.7	803.4	846.1	878.4	333.7	786.3	809.6	288.9	360.5	827.5	760.7	740.3
	6	820.4	817.4	917.3	874.7	822.4	801.6	683.6	394.4	516.6	669.9	772.5	735.2
	7	814.0	820.1	850.7	895.1	681.6	224.0	776.0	787.9	140.5	784.5	792.6	736.0
	8	823.9	815.2	850.4	861.2	826.7	710.1	588.7	390.3	884.3	840.0	716.3	742.4
	9	792.7	894.8	840.0	871.8	839.5	824.8	427.3	553.0	828.3	212.7	653.3	729.3
	10	802.8	818.6	869.2	865.0	895.1	802.8	756.5	213.7	860.2	637.7	768.9	597.0

	11	810.3	824.3	836.9	860.7	835.9	797.4	734.1	51.7	264.6	862.8	787.5	757.2
	12	819.8	534.1	852.9	857.6	821.0	713.3	823.2	819.7	819.9	794.5	740.3	739.7
	13	815.7	444.3	808.9	853.5	903.6	837.4	201.6	360.3	116.6	840.0	771.1	761.3
	14	780.5	648.8	939.9	834.3	470.1	718.9	769.6	370.6	142.5	862.3	781.3	741.0
	15	716.5	745.8	859.5	862.9	420.6	820.5	795.5	236.0	656.5	747.2	787.7	721.4
	16	773.0	809.0	753.0	856.1	584.3	778.1	737.9	563.3	719.4	803.9	777.1	738.3
	17	782.4	802.3	429.3	882.3	867.2	767.1	706.1	878.8	849.5	841.1	772.9	717.6
	18	788.5	202.7	866.3	836.5	363.6	603.5	585.9	660.8	839.1	771.9	678.2	711.9
	19	779.9	808.6	874.0	832.7	829.1	175.6	810.5	675.6	960.7	520.0	762.9	721.8
	20	777.4	849.9	829.0	667.9	809.9	757.0	770.3	853.9	222.8	675.2	769.8	730.1
	21	775.1	856.3	789.3	882.1	680.8	115.5	753.4	443.1	885.5	822.1	754.1	740.7
	22	769.8	819.3	795.3	873.7	594.7	717.4	724.8	746.1	357.1	810.2	755.5	756.2
	23	818.3	856.0	784.0	772.7	820.6	763.8	789.9	744.4	785.2	798.8	738.0	754.4
	24	812.1	839.1	842.9	853.1	584.2	803.8	784.4	176.4	855.1	808.3	711.9	755.2
	25	819.9	818.5	844.7	837.7	800.8	699.4	652.7	883.1	699.2	582.3	732.1	787.6
	26	809.7	817.0	854.9	470.9	791.7	758.0	463.1	367.4	834.6	808.0	769.0	769.9
	27	830.1	835.8	857.3	941.8	685.0	775.2	813.3	923.1	819.1	812.5	754.9	731.3
	28	821.4	842.0	839.8	240.6	630.1	781.8	671.7	909.2	829.1	809.7	726.7	741.6
	29	811.1		880.9	713.1	816.8	783.9	797.3	208.1	851.2	798.4	731.5	746.1
	30	793.2		847.1	796.9	138.3	863.2	785.6	586.9	869.0	811.7	751.3	738.9
	31	788.4		854.7		802.3		547.0	825.1		798.1		732.6
2018	1	747.1	737.2	863.8	857.0	833.4	703.3	760.8	794.4	807.2	815.4	772.9	NA
	2	703.9	739.8	848.5	505.0	865.2	812.1	733.3	650.2	866.1	346.0	509.2	NA
	3	684.5	728.4	824.0	872.4	859.8	889.7	619.5	808.0	802.4	850.6	765.6	NA
	4	717.1	764.1	829.0	801.9	850.0	800.0	380.2	871.4	738.4	815.0	773.0	NA
	5	715.2	782.8	833.1	749.6	849.6	781.3	688.5	632.0	200.0	822.3	342.0	NA
	6	695.1	793.3	767.2	857.8	804.5	793.0	872.0	668.4	630.6	803.7	690.4	NA
	7	723.7	793.8	826.9	850.5	768.0	783.2	611.5	442.6	592.4	727.2	799.1	NA
	8	735.0	794.9	853.1	852.9	841.4	798.3	756.3	473.1	815.1	654.2	307.6	NA
	9	724.9	789.2	867.2	878.8	849.1	809.2	750.1	782.0	657.8	544.7	710.0	NA

	10	722.3	784.9	862.8	873.9	797.0	776.4	591.3	404.8	913.0	610.9	245.4	NA
	11	730.4	808.3	845.6	871.8	809.7	767.4	751.6	668.4	836.1	781.0	752.0	NA
	12	734.8	790.5	843.8	863.7	801.3	739.9	743.8	192.7	843.0	791.5	764.8	NA
	13	770.9	789.4	852.3	856.9	823.6	672.5	786.0	508.8	609.2	835.6	782.4	NA
	14	782.2	789.3	833.5	837.1	802.3	325.7	767.3	795.5	833.2	852.8	752.8	NA
	15	793.2	786.2	853.2	832.0	836.4	801.4	744.1	703.9	822.3	836.9	324.9	NA
	16	763.8	669.6	857.0	853.9	805.3	749.3	763.5	629.2	847.5	811.7	549.4	NA
	17	756.5	780.7	869.9	903.2	781.0	759.9	689.6	822.0	820.4	478.4	578.6	NA
	18	735.5	808.6	859.9	834.5	816.2	772.0	141.4	471.8	91.4	811.0	749.3	NA
	19	727.0	909.2	853.6	412.4	838.4	767.5	534.0	911.0	824.2	781.1	749.7	NA
	20	733.1	853.1	855.3	416.7	586.8	701.4	549.6	745.6	472.9	459.6	769.1	NA
	21	728.2	835.3	859.5	838.2	840.4	730.9	383.0	817.8	790.6	805.0	774.9	NA
	22	721.2	875.2	856.1	487.4	469.9	737.7	604.3	859.4	822.3	744.1	759.7	NA
	23	740.9	562.9	862.1	532.1	624.4	739.0	234.1	824.1	834.1	773.2	738.8	NA
	24	757.4	559.2	860.9	934.8	495.4	742.0	391.0	926.1	836.7	795.6	738.0	NA
	25	735.6	851.4	850.8	801.2	809.2	234.9	770.8	823.8	682.3	808.3	732.3	NA
	26	780.3	829.7	860.0	838.7	584.5	644.6	866.6	625.3	819.8	795.2	737.4	NA
	27	753.3	826.4	850.8	808.2	783.3	724.3	786.7	420.2	773.7	789.3	NA	NA
	28	743.9	841.4	839.5	830.7	777.1	760.4	859.0	831.1	731.3	789.3	NA	NA
	29	758.8		845.5	851.9	364.9	681.6	331.2	639.5	815.4	787.1	NA	NA
	30	743.8		852.7	842.2	141.8	721.6	848.5	667.2	353.7	363.0	NA	NA
	31	741.6		825.9		743.5		789.2	859.5		773.0		NA

NASA Surface meteorology data

	Unit	Climate data location						
Latitude	°N	-9.39						
Longitude	°E	-11.954						
Elevation	m							
Heating design temperature	°C	23.9						
Cooling design temperature	°C	26.83						
Earth temperature amplitude	°C	1.01						
Frost days at site	days	0						
Month	Air Temperature °C	Relative Humidity %	Daily Solar Radiation-Horizontal $kwh/m^2/d$	Atmospheric Pressure *kpa*	Wind Speed m/s	Earth Temperature °C	Heating Degree-Days °C − *d*	Cooling Degree-Days °C − *d*
January	25.2	73.5	7.74	101.3	6.2	26.1	0	470
February	25.7	75.2	7.60	101.2	5.7	26.6	0	445
March	26.3	76.3	7.01	101.2	5.6	27.2	0	505
April	26.6	75.8	6.43	101.2	5.8	27.5	0	496
May	26.3	75.0	5.91	101.2	6.2	27.3	0	504
June	25.9	74.0	5.46	101.3	6.3	26.9	0	475
July	25.2	73.0	5.63	101.4	6.9	26.2	0	471
August	24.8	72.6	6.33	101.4	6.7	25.6	0	457
September	24.6	73.1	7.01	101.4	6.3	25.5	0	436
October	24.5	73.3	7.55	101.4	6.2	25.5	0	447
November	24.5	72.9	7.74	101.3	5.8	25.6	0	435
December	24.8	73.1	7.64	101.3	5.8	25.9	0	458
Annual measured	25.4	74.0	6.84	101.3	6.1	26.3	0	5599

Thermal properties of thermal oil heat transfer fluid

Temperature	Liquid density	Liquid heat capacity	Liquid thermal conductivity	Liquid viscosity	Vapor pressure
	kg/m3	$(kJ/kg.K)$	$W/(m \cdot K)$	$cSt\ (mm2/s)$	kPa
–20	1056	1.495	0.127	908	—
–10	1049	1.527	0.126	299	—
0	1042	1.559	0.125	125	—
10	1034	1.592	0.124	61.2	—
20	1027	1.624	0.124	34.0	—
30	1020	1.656	0.123	20.7	—
40	1013	1.688	0.122	13.6	—
50	1006	1.721	0.121	9.45	—
60	998	1.753	0.120	6.89	0.033
70	991	1.785	0.120	5.22	0.057
80	983	1.817	0.119	4.08	0.094
90	976	1.849	0.118	3.27	0.151
100	969	1.882	0.117	2.69	0.237
110	962	1.914	0.116	2.25	0.365
120	955	1.946	0.116	1.91	0.551
130	947	1.978	0.115	1.65	0.814
140	940	2.011	0.114	1.44	1.18
150	933	2.043	0.113	1.27	1.69
160	926	2.075	0.112	1.14	2.38
170	919	2.107	0.112	1.02	3.30
180	911	2.140	0.111	0.927	4.52
190	904	2.172	0.110	0.846	6.10
200	898	2.204	0.109	0.777	8.15
210	890	2.236	0.108	0.718	10.8
220	883	2.269	0.107	0.666	14.0
230	876	2.301	0.107	0.622	18.1
240	869	2.333	0.106	0.582	23.2
250	862	2.365	0.105	0.547	29.5
260	854	2.398	0.104	0.516	37.1
270	847	2.430	0.103	0.489	46.3
280	840	2.462	0.103	0.464	57.3
290	833	2.494	0.102	0.441	70.5
300	826	2.527	0.101	0.421	86.1
310	818	2.559	0.100	0.403	104
320	811	2.591	0.099	0.386	126
330	804	2.623	0.099	0.371	151
340	797	2.655	0.098	0.357	180
350	790	2.688	0.097	0.344	213
360	782	2.720	0.096	0.332	251